The epigenetic eraser LSD1 lies at the apex of a reversible erythroid to myeloid cell fate decision

Lei Yu[1], Greggory Myers[1,2], Chia-Jui Ku[1], Emily Schneider[1], Yu Wang[1], Sharon A. Singh[3], Natee Jearawiriyapaisarn[4], Andrew White[5], Takashi Moriguchi[6], Rami Khoriaty[1,2], Masayuki Yamamoto[1,7], M. Geoffrey Rosenfeld[8], Julien Pedron[9], John H. Bushweller[9], Kim-Chew Lim[1], James Douglas Engel[1*]

[1]Departments of Cell and Developmental Biology, [2]Internal Medicine and [3]Pediatrics and Infectious Diseases, University of Michigan Medical School, Ann Arbor, MI 48109;

[4]Thalassemia Research Center, Institute of Molecular Biosciences, Mahidol University, Nakhon Pathom, Thailand;

[5]Vahlteich Medicinal Chemistry Core, College of Pharmacy, University of Michigan;

[6]Tohoku Medical and Pharmaceutical University, Sendai, Japan;

[7]Tohoku Medical Megabank Organization, Tohoku University, Sendai, Japan;

[8]Department of Medicine, University of California San Diego School of Medicine;

[9]Department of Molecular Physiology and Biological Physics, University of Virginia School of Medicine.

[*]Corresponding author

3035 BSRB, 109 Zina Pitcher Place

Ann Arbor, MI 49109

Email: engel@umich.edu

Telephone: 734-647-0803

Abstract (250 words)

Histone H3 lysine 4 methylation (H3K4Me) is proximally associated with chromatin activation, and therefore removing H3K4 methyl groups is normally coincident with gene repression. H3K4Me demethylase KDM1a/LSD1 is a potential therapeutic target for multiple diseases, including for the treatment of the β-globinopathies (sickle cell disease and β-thalassemia) since it is a component of multiple γ-globin repressor complexes, and its inactivation leads to robust induction of the fetal globin genes. However, the effects of LSD1 inhibition in definitive erythroid cells are not well characterized. Here we examined the consequences of erythroid-specific conditional inactivation of *Lsd1 in vivo* using a new *Gata1*^{creERT2} bacterial artificial chromosome (BAC) transgene. Conditional loss of *Lsd1* in adult mice led to a differentiation block in erythroid progenitor cells and the surprising expansion of a GMP-like cell pool, apparently converting hematopoietic differentiation potential from an erythroid to a myeloid fate. The analogous phenotype was also observed in human cells: inactivation of LSD1 in hematopoietic stem and progenitor cells (HSPC) also blocked erythroid differentiation, coincident with robust induction of myeloid transcription factor genes (*e.g*. *Pu.1* and *Cebpa*). Remarkably, blocking the activity of PU.1 or RUNX1 (a transcriptional activator of *Pu.1*) at the same time as blocking LSD1 activity reverted the myeloid lineage conversion back to an erythroid phenotype. Taken together, the data show that LSD1 maintains erythropoiesis by reversibly repressing a myeloid cell fate in adult erythroid cell precursors, and that inhibition of the myeloid differentiation pathway can reverse the negative effects of LSD1 inactivation on erythroid differentiation.

Introduction

Sickle cell disease (SCD) is a genetic disorder arising from a single nucleotide transversion, resulting in a Glu to Val amino acid change in the human β-globin protein, β^s. β^s subunits comprise equal parts, with α-globin subunits, of the tetrameric human hemoglobin, HbS [$\alpha_2\beta_2^S$]. HbS polymerizes in hypoxic red blood cells (RBC) causing RBC sickling, increased fragility and subsequent destruction, thereby leading to pathological organ damage, episodic acute pain and early death in affected individuals[1,2]. Clinical studies showed that the pathophysiological severity of SCD negatively correlates with increased levels of fetal hemoglobin (HbF; $\alpha_2\gamma_2$)[2]. β-thalassaemia major (TM; aka Cooley's Anemia, CA) can arise by biallelic inheritance of any of hundreds of different recessive genetic mutations leading to diminished or altered expression of the adult β-globin gene[3]. However, co-inheritance of hereditary persistence of fetal hemoglobin (HPFH) alleles, normally leading to a benign hematopoietic condition characterized by elevated HbF levels in adults, significantly ameliorates SCD and TM disease pathology, making HbF re-activation in adults a focal therapeutic target for treating the β-globinopathies[4-8]. The beneficial effect of increased HbF levels on RBC longevity and stability in SCD has been confirmed in cell culture studies as well as in multiple animal models[9].

The human β-globin locus spans more than 70 kb on chromosome 11 and is composed of five genes that are sequentially transcribed during development[10]. Spatially located from closest to farthest from the locus control region (LCR)[11,12], the five genes are arranged in their temporal order of developmental expression: ε- [embryonic], Gγ- and Aγ- [fetal], and δ- and β-globin [adult]. The switch from ε- to γ-globin transcription occurs as definitive erythropoiesis initiates in the fetal liver. At around the time of birth, γ-globin is gradually silenced and active transcription "switches" predominantly to the adult β-globin gene[13]. The competition model was proposed as the earliest explanation for a mechanism that might control globin gene switching[14], and suggested that each of the globin genes competes for the *trans*-activating activity of the LCR super-enhancer[13]. According to this hypothesis, the

globin gene closest to the LCR would have a greater chance to interact with the LCR and therefore are actively transcribed, unless a linearly closer gene is repressed by gene-autonomous silencing[15-20]. Thus, a more comprehensive mechanistic understanding for how the γ-globin genes are regulated in adult erythroid cells could provide crucial conceptual insights into how HbF might be reactivated, by either genetic or pharmacological means, for therapeutic benefit in the erythroid cells of TM and SCD patients.

Extensive effort has focused on the mechanisms that regulate γ-globin autonomous repression/gene silencing in adult red blood cells. Most notably, mutations in the binding sites for multiple transcription factors (TFs) in the vicinity of the γ-globin gene result in functional hereditary persistence of fetal hemoglobin (HPFH)[9]. These TFs include Bcl11a, LRF, GATA1 and an orphan nuclear receptor heterodimer composed of TR2 and TR4[21,2223,24]. We previously reported that TR2/TR4 directly binds to the γ-globin promoter to recruit a multimeric Direct Repeat Erythroid-Definitive (DRED) multi-subunit protein complex to repress γ-globin transcription in adult erythroid cells[21,22]. The core co-repressor subunits of both the DRED complex and BCL11a include a scaffold protein, NCoR1, which recruits the epigenetic chromatin modifying enzymes DNMT1 and LSD1, among several others[25-27].

LSD1/KDM1A is a flavin adenine dinucleotide-dependent histone demethylase that is specific for methylated histone H3 lysine 4 and 9 (H3K4 and H3K9)[28,29]. Pharmacological inhibition of LSD1 de-represses HbF synthesis by up to 30% in cell cultures of erythroid differentiated human HSPC[27], which is a level widely acknowledged to be of significant potential therapeutic benefit to SCD or TM patients. *In vivo* administration of one LSD1 inhibitor, RN-1, to baboons, an animal model with a globin gene expression profile that closely resembles human developmental expression, robustly re-activated HbF synthesis [30,31]. Additionally, RN-1 administration to humanized SCD model mice was shown to re-activate HbF synthesis and significantly ameliorate the pathological characteristics of SCD[32]. Taken together, the data indicate that safe, efficient LSD1 inhibition would be efficacious for

HbF induction in humans, and as a widely accessible treatment for SCD and TM by millions of affected individuals worldwide.

Given the promising effect of LSD1 inhibitors in HbF induction *in vitro* and *in vivo*, it would be important to understand in preclinical studies any adverse effects of LSD1 inhibition by drug candidates in adult erythroid cells. Pan-hematopoietic *Lsd1* deletion using Mx1Cre[33] or inducible RNAi-based LSD1 mRNA knockdown[34] in adult mice impaired erythropoiesis coupled to an expansion of HSPC, suggesting that LSD1 plays an active role in multiple hematopoietic lineages, and not solely in erythropoiesis. Therefore, a detailed mechanistic understanding of how LSD1 inhibition affects adult hematopoiesis would be critical to address the potential therapeutic and adverse effects of any candidate LSD1 inhibitor for clinical use.

In this study, we generated an erythroid-inducible Cre mouse line by modifying a mouse *Gata1* BAC that would allow us to conditionally investigate functions of LSD1 in adult murine erythroid cells. During the analysis of erythroid-specific *Lsd1* conditional loss-of-function (LOF) mice, we discovered that this epigenetic modifying enzyme plays a key role in repressing myeloid gene expression. Erythroid-specific *Lsd1* inactivation *in vivo* led to a marked expansion of granulocyte-monocyte progenitor (GMP)-like cells in the bone marrow, and surprisingly these novel GMPs arise from erythroid progenitor (EP) cells. Furthermore, PU.1, a key transcription factor required for myeloid differentiation, was significantly induced in colony forming unit-erythroid (CFU-E) cells recovered from *Lsd1*-CKO mouse bone marrow. In a similar manner, pharmacological inactivation of LSD1 in human CD34+ HSPC that were induced to undergo erythroid differentiation significantly re-activated myeloid genes (*Pu.1, Cebpa* and *Runx1*) to severely impair erythroid differentiation. Finally, co-inactivation of *Lsd1* and either *Pu.1* or *Runx*1 partially rescued the erythroid cytotoxicity associated with LSD1 inhibition. Taken together, the data indicate that LSD1 functional loss impairs erythropoiesis through a reversible mechanism that induces the activation of a myeloid gene expression program in erythroid progenitors leading to an erythroid to myeloid cell fate conversion. Furthermore, the data show that inhibition of the RUNX1/PU.1 myeloid

differentiation axis allows fetal hemoglobin induction in the absence of the LSD1 LOF-induced block in erythroid differentiation.

Results

LSD1 inhibitors induce HbF but block erythroid differentiation

Current LSD1 inhibitors, exemplified by tranylcypromine (TCP), are all small chemical compounds that initially showed promising potential for use as SCD therapeutics because of their ability to stimulate fetal γ-globin expression to high levels[27]. However, all of the commercial inhibitors that we have tested to date exhibit one or more properties that prohibits their use as promising drug candidates. One novel LSD1 inhibitor that we recently synthesized, CCG50, is a small organic molecule that was designed to bind reversibly to the flavin-dependent catalytic center of LSD1 (data not shown), thus differing from the majority of current (irreversible) commercial inhibitors. We showed that CCG50 (referred to interchangeably as LSD1i) efficiently and specifically inhibited LSD1 function with an IC_{50} of 115 nM (Supplemental Fig. 1A).

To test whether LSD1i administration would, like TCP, also induce abundant γ-globin expression, we tested erythroid differentiation in human CD34+ HSPC using a standard three-phase culture system (Supplemental Fig. 1B)[35,36]. To score erythroid differentiation progression, we monitored CD71 (transferrin receptor) and CD235a (glycophorin A) expression beginning on d7 (prior to LSD1i addition) and again on d11, d14 and d18 by flow cytometry. In this culture system, proerythroblasts first acquire CD71 followed by CD235a surface antigens and subsequently lose CD71 expression to finally display only CD235a as mature erythroid cells[36,37]. A minority of such HSPC remained double negative (15%) while most cells had acquired one (14% CD71) or both (70% CD71 + CD235a) erythroid differentiation antigens by d7 (Supplemental Fig. 1C). After differentiation induction on d7 (following the removal of hydrocortisone and human IL3), over 90% of control cells treated with DMSO alone expressed both of these erythroid cell surface markers by d11 and d14, while by d18, 20% of the cells had lost CD71 expression to finally become CD235a singly-positive mature erythroid cells (DMSO panels, Fig. 1A). At the lowest LSD1i concentration tested (120 nM), the flow cytometric pattern of cells at d11 (last column, Fig. 1A) resembled

that of d7 controls (Supplemental Fig. 1C) with the majority (65%) of cells remaining double-positive erythroid precursors. From d14 through d18, the majority (95%) of cells remained CD71+ CD235a+ with only 3-4% converting to more mature CD71- CD235a single positive cells. In contrast, at the highest concentration of LSD1i tested (1.1 μM), most of the cells (>70%) remained double negative even by d18 (Fig. 1A). Hence, the novel, reversible LSD1 inhibitor CCG50 exhibits the same concentration-dependent inhibitory effect on erythroid differentiation that was also observed with other LSD1 inhibitors, including RN-1 and TCP (data not shown).

Next, we assessed HbF synthesis by HPLC analysis of the hemoglobins produced in d18 differentiated erythroid cells cultured in the presence or absence of LSD1i. At all three concentrations tested (120 nM, 370 nM or 1.1 μM), LSD1i induced γ-globin synthesis and HbF above the baseline level of 2.5% (in DMSO mock-treated control cells) to between 10.8% and 24.4% (Fig. 1B). Globin mRNA analysis indicated that although LSD1i enhanced the γ/(γ+β) ratio in a dose-dependent manner (Fig. 1C), total β-like globin (γ+β) mRNA significantly declined and negatively correlated with increasing LSD1i concentration (Fig. 1D). As anticipated, expression of several key erythroid transcription factors (GATA1, KLF1 and TAL1) was also reduced after LSD1i administration (Fig. 1E). Taken together, the data indicate that while low to moderate LSD1 inhibition (at 120 or 370 nM CCG50) robustly induced HbF, while higher concentrations significantly impaired erythroid differentiation accompanied by increased cytotoxicity in *ex vivo* expanded human CD34+ HSPC.

Generation of conditional, erythroid lineage-specific deleter transgenic mice

We next investigated whether genetic *Lsd1* LOF *in vivo* would similarly inhibit adult erythroid differentiation in a mouse model. While Mx1-Cre[38], EpoR-Cre[39], and Vav1-Cre[40] deleter strains have been utilized in the past to achieve pan-hematopoietic or erythroid-specific recombination of loxP-flanked genes *in vivo*, none were ideal for generating conditional LOF alleles (CKO) in adult murine red blood cells, as Cre activity is either not

inducible (*e.g*. in EpoR-Cre or Vav1-Cre animals), or is not restricted solely to the erythroid lineage (Vav1-Cre and Mx1-Cre). To circumvent this issue, we generated and characterized erythroid lineage-specific, tamoxifen (Tx)-inducible lines of Cre transgenic mice to determine the *in vivo* effect(s) of *Lsd1* LOF during definitive erythropoiesis in adult animals.

We utilized a 196 kb mouse *Gata1* Bacterial Artificial Chromosome (abbreviated *G1B*) as the Cre delivery vehicle, which we had previously shown to faithfully recapitulate endogenous mouse *Gata1* gene expression[41-43]. A tamoxifen (Tx)-inducible CreER^{T2} fusion gene[44], encoding a Cre recombinase whose activity is dependent on the binding of the Tx ligand, was inserted at the ATG start codon of the *Gata1* BAC by gene editing (Supplemental Fig. 2). Correctly targeted *G1B*CreER^{T2}-Neo+ clones were verified by PCR (not shown). The *frt*-flanked Neo selection marker was subsequently excised from the BAC by activating L-arabinose-induced Flp recombinase expression in EL250 cells[41]. The resultant modified *G1B*CreER^{T2} BAC clones were verified by PCR and finally by Sanger sequencing (not shown). The BAC was then microinjected into C57Bl/6J zygotes to generate transgenic mice, from which two *G1B*CreER^{T2} transgenic lines, L245 and L259, were recovered.

To determine the tissue specificity and activity of Cre recombinase in the two *G1B*CreER^{T2} mouse lines, we crossed them to the *Rosa26*-loxP-Stop-loxP-TdTomato (*R26T*) reporter mouse to generate compound *R26T:G1B*CreER^{T2} mutant mice, in which TdTomato (TdT) expression is activated upon Cre-mediated deletion of the loxP site-flanked transcriptional stop cassette[45]. *R26T:G1B*CreER^{T2} mice were injected with Tx every other day five consecutive times; untreated *R26T:G1B*CreER^{T2} mice were included as negative controls. Two weeks after the first Tx administration, total bone marrow (BM) cells were collected to analyze TdT epifluorescence in cells of the hematopoietic hierarchy. Total BM cells from control and Tx-treated mice were separately co-stained with anti-CD71 and -Ter119 antibodies to monitor erythroid differentiation.

As erythroid cells mature, they first acquire CD71 expression (gate II; Fig. 2A) before co-expressing both Ter119 and CD71 (gate III) and then gradually lose CD71 immunopositivity

(gate IV) to express Ter119 alone (gate V)[46]. No TdT signal was detected in the BM of either L245 or L259 mice that were not administered Tx, indicating that CreER^{T2} activity was not "leaky" (blue peaks, Fig. 2B). Since CreER^{T2} was under the transcriptional control of *Gata1 cis*-regulatory elements contained within the 196 kb BAC, we expected that upon Tx administration, only cells with erythroid developmental potential would express TdT. Indeed, fraction I, which primarily represents BM non-erythroid cells, were almost exclusively TdT-negative, whereas > 90% of the cells in fraction II, which are committed to erythroid differentiation, were labeled by TdT (Fig. 2B, red peaks). Notably, the TdT intensity diminished as cells differentiated (fractions III-V), likely due to some combination of global erythroid nuclear condensation, TdT turnover and dilution (Fig. 2B). We also stained whole BM cells with a cocktail of antibodies recognizing non-erythroid hematopoietic cell surface antigens to determine whether CreER^{T2} expression was expressed in B (B220), T (CD3e) or myeloid (Gr1, CD11b) cell lineages. Flow cytometry indicated that very few TdT+ cells were present in the B220/Gr1/CD11b/CD3e+ population (Supplemental Fig. 3, red peak), indicating that the *G1B*CreER^{T2} transgene was active essentially only in erythroid lineage cells. Both transgenic lines L245 and L259 shared similar TdT expression profiles (Fig. 2B and Supplemental Fig. 3), and therefore only line L259 was used for all subsequent studies.

Since the mouse *Gata1* gene is known to be expressed in megakaryocytes (Mk), and other myeloid cells[47], we examined Cre activity in Mk progenitors (MkPs), Mk and mast cells in *R26T:G1B*CreER^{T2} mice (Supplemental Figs. 4 and 5). Only 10% of MkP (defined as Lin-cKit+Sca1-CD41+CD150+) (Supplemental Figs. 4A, 4B and 5) and 25% of mature CD41+CD61+ Mk cells were TdT+ (Supplemental Figs. 4C, 4D). Of the FcRIa+c-Kit+ mast cells, 15% were TdT+ (Supplemental Figs. 4E, 4F). These data suggested that either the *G1*BAC does not contain the *Gata1* regulatory element(s) that are required for expression in Mk and mast cells or that endogenous GATA1 is expressed in only a subset of those lineages. Taken together, the data indicate that the *G1B*CreER^{T2} mouse is a novel, inducible genetic tool that is faithfully expressed in the erythroid lineage.

Hematopoietic lineage expression of *G1B*CreER^{T2}

We next investigated the expression of *G1B*CreER^{T2} within the early hematopoietic hierarchy. Total BM cells were harvested from *R26T:G1B*CreER^{T2} mice that were either injected with Tx or corn oil (control) and then stained with antibodies for Lin-Sca1+c-Kit+ (LSK cells, murine hematopoietic stem and progenitor cells), common myeloid progenitors (CMP: Lin-c-Kit+Sca1-CD34+CD16/32-), granulocyte-monocyte progenitors (GMP: Lin-c-Kit+Sca1-CD34+CD16/32+), megakaryocyte-erythrocyte progenitors (MEP: Lin-c-Kit+Sca1-CD34-CD16/32-) or colony forming unit-erythroid cells (CFU-E: Lin-c-Kit+Sca1-CD41-CD16/32-CD150-CD105+) using conventional cell surface markers to identify each subpopulation[48] (Supplemental Figs. 5-7, Fig. 2C). Of the LSK cells, approximately 5% were TdT+ after Tx-induced CreER^{T2} activation, which may represent an erythroid- or Mk-primed progenitor cell population (Fig. 2C, red peak)[49]. As anticipated, no CMP or GMP cells were labeled after Tx administration (Fig. 2C). In contrast, 85% of MEP and 90% of CFU-E were TdT+ (Fig. 2C). In summary, the data indicate that the Cre activity of *G1B*CreER^{T2} mice can be detected as early as the MEP stage of erythroid developmental commitment as well as at all subsequent stages of erythroid differentiation.

Erythroid progenitor deficiencies in *Lsd1* CKO mice

In previous studies using EpoR Cre to facilitate erythroid lineage-specific *Lsd1* ablation, Kerenyi *et al.*[33] reported prenatal lethality as a result of defective erythropoiesis. To investigate the effects of *Lsd1* conditional erythroid ablation in adult animals, we intercrossed *G1B*CreER^{T2} L259 mice with *Lsd1* homozygous floxed (*Lsd1*$^{f/f}$) mice[50], all in a congenic C57Bl/6 background, to generate compound mutants. *Lsd1*$^{f/f}$:*G1B*CreER^{T2} (*Lsd1* CKO) or *Lsd1*$^{+/+}$:*G1B*CreER^{T2} (control) mice were administered Tx seven times every other day for two weeks. Mice were sacrificed for hematological analysis 12 hours after the final Tx injection, unless otherwise noted. This strategy increased the possibility that erythroid progenitor cells, when continuously exposed to Tx, might more likely delete *Lsd1* in progenitors that had escaped earlier Cre-mediated inactivation.

Peripheral blood differential analysis indicated that the *Lsd1* CKO mice suffered from anemia, as all erythroid parameters were significantly affected (Table 1). In contrast, the WBC count was indistinguishable between the *Lsd1* CKO and control groups. Somewhat surprisingly, platelet counts were significantly higher in the *Lsd1* CKO mice (Table 1), consistent with the increase in the number of CD41+ Mks in the BM of *Lsd1* CKO mice (data not shown).

To investigate the source of the anemia observed in the *Lsd1* CKO mice in greater detail, we performed *in vitro* colony assays of total BM cells from Tx-treated *Lsd1* CKO and control mice. The data indicated that colony-forming unit-granulocyte, erythroid, monocyte, megakaryocyte (GEMM or CFU-GEMM) numbers were indistinguishable between the *Lsd1* CKO and control animals (Fig. 3A). Interestingly, there were slightly, but significantly, more colony-forming unit-granulocyte, monocyte (GM or CFU-GM) colonies in *Lsd1* CKO BM (Fig. 3A). Among committed erythroid progenitor populations, both burst-forming unit-erythroid (BFU-E) and CFU-E were quantitatively (by 50% or 90%, respectively; Fig. 3A) and qualitatively reduced (Fig. 3B) compared to control BM progenitors, thus indicating a severe depletion in the erythroid progenitor populations as a result of *Lsd1* ablation. Hence, the anemia observed in *Lsd1* CKO mice stemmed from a severe reduction in the number of erythroid progenitor cells.

We did not observe splenomegaly in *Lsd1* CKO mice, suggesting that erythroid progenitors responsible for extramedullary hematopoiesis were also affected (Fig. 3C). In agreement with the results of the CFU colony assays, flow cytometry showed that the absolute number of CFU-E in *Lsd1* CKO mice was significantly reduced, by approximately 70%, when compared to controls (Fig. 3D, E). Based on AnnexinV staining results[51], this reduction was not attributable to increased programmed cell death of CFU-E (Supplemental Fig. 8). Taken together, the data indicate that *Lsd1* LOF leads to a severe block in generating a normal number of erythroid progenitor cells, most markedly at the CFU-E stage, and consequentially to fewer circulating mature red blood cells, and that decrease is not due to increased erythroid cell death.

In the *Lsd1* CKO BM, the number of CD71+Ter119+ erythroid precursor cells was significantly lower than in control BM (6.5% vs 24%; Fig. 3F). CD71+ erythroid precursor cells can be further fractionated into progressively more mature basophilic erythroblasts (BasoE), polychromatic erythroblasts (PolyE) and orthochromatic erythroblasts (OrthoE) using a CD44+ vs. forward scatter (FSC) flow cytometry gating strategy (Fig. 3F)[46]. The absolute cell number of BasoE, PolyE and OrthoE were all significantly reduced in the *Lsd1* CKO CD71+Ter119+ BM (Fig. 3F, G), and the >70% reduction in erythroid precursor cells was likely due to continuous differentiation dysfunction that can first be detected in BFU-E cells (Fig. 3A, E).

To test the possibility that the residual erythroid precursor cells in the treated animals were not simply cells that had escaped *Lsd1* conditional deletion, we quantified Cre-mediated deletion efficiency in flow-sorted BasoE. A primer pair that was designed to amplify the *Lsd1* genomic region predicted to be lost after excision between the loxP sites (P1), and the product was normalized a the control primer amplicon (P2) that amplified intact genomic DNA lying adjacent to the loxP sites (Fig. 3H). The data show that >80% of FACS-sorted BasoE had deleted the genomic DNA between the two loxP sites (Fig. 3H). Hence, *G1B*CreER^{T2} achieved highly efficient conditional *Lsd1* inactivation in adult erythroid lineage cells.

During erythroid cell maturation, there is normally an exuberant increase in cell numbers as erythroid precursor cells transit from basophilic to polychromatic to orthochromatic erythroblasts, as observed in the control mice (Fig. 3G, gray bars). However, in *Lsd1* CKO mice, the cell numbers increased only marginally between the basophilic and orthochromatic cell stages (Fig. 3G, black bars). This difference in differentiation potential between *Lsd1* CKO and control mice indicates that LSD1 plays an important role in maturation at multiple sequential stages during erythroid cell differentiation.

We next asked whether increased cell death might account for the observed deficiency in erythroid precursor cells in *Lsd1* CKO mice. Early and late apoptotic cells (AnnexinV+DAPI- and AnnexinV+DAPI+, respectively[41]) were analyzed in BasoE, PolyE and

OrthoE cells in *Lsd1* CKO and control mice. Surprisingly, the late apoptotic frequency of both BasoE and PolyE in *Lsd1* CKO mice was significantly reduced (to approximately half), whereas cell death of OrthoE in *Lsd1* CKO mice was unchanged (Supplemental Fig. 9). Furthermore, the cell cycle in the CD71+Ter119+ precursor population was unaffected when comparing *Lsd1* CKO and control mice (Supplemental Fig. 10). Taken together, the data indicate that *Lsd1* LOF blocks the differentiation of erythroid precursor cells in a manner that is independent of programmed cell death or alterations in the cell cycle.

***Lsd1* CKO erythroid progenitors acquire myeloid characteristics**

The data presented thus far indicates that *Lsd1* conditional LOF results in marked depletion of definitive erythroid progenitor and precursor cells that is independent of cell cycle and cell death. Curiously, data from the colony assays showed that the GM colony number was slightly but significantly increased (Fig. 3A). To potentially explain this curious observation we hypothesized that erythroid progenitor cells might have acquired myeloid features through a lineage switch that reciprocally impaired erythroid potential. To test this hypothesis, we examined the LSK, CMP, MEP and GMP progenitor cell populations in *Lsd1* CKO and control mice (Fig. 4A-B and Supplemental Fig. 7); the data show that the absolute numbers of LSK, CMP and MEP were comparable among the groups. However, consistent with the hypothesis that erythroid progenitors were being diverted into other hematopoietic lineages, the GMP population significantly increased in the *Lsd1* CKO BM (Fig. 4A, 4B). Curiously, we also detected prominent expansion of a new Lin-c-Kit+Sca1-CD16/32+CD34- cell population in the *Lsd1* CKO bone marrow when compared to control mice (Fig. 4A).

To test whether the expanded GMP population in *Lsd1* CKO mouse BM might arise from erythroid lineage origin, we generated *Lsd1*$^{f/f}$*:G1B*CreER^{T2}:*R26T* triple mutant mice (hereafter referred to as *Lsd1* CKOT) in order to lineage trace TdT fluorescence in the expanded GMP population discovered in the *Lsd1* CKO mice. Since the erythroid cells, but not GMP cells, in *G1B*CreER^{T2}:*R26T* mice were labeled by TdT (Fig. 2C), we reasoned that the surfeit GMP cell population in *Lsd1* CKOT mice would be TdT+ if they were in fact

derived from erythroid precursor cells. As expected, LSK or MEP populations in either Tx-treated control (*R26T*:*G1B*CreER^{T2}) versus *Lsd1* CKOT mice were TdT- or TdT+, respectively (Fig. 4C), consistent with earlier observations (Fig. 2C). In Tx-treated *R26T*:*G1B*CreER^{T2} control mice, GMP cells were not labeled by TdT (Fig. 2C). Notably, and consistent with the observed three-fold increase in GMP cell number (Fig. 4A, 4B), 60% of GMP cells in *Lsd1* CKOT mice were TdT+ (Fig. 4C). Based on detailed characterization of hematopoietic TdT expression (Fig. 2 and Supplemental Figs. 3 and 4), we conclude that these LSD1-deficient TdT+ GMP cells must originate from an erythroid progenitor population.

We next asked whether the GMP population in *Lsd1* CKO mice (Fig. 4B) might be differentially susceptible to programmed cell death. While the early apoptotic populations of GMP were comparable in *Lsd1* CKO and control groups, late apoptosis was reduced by 50% in the *Lsd1* CKO GMP fraction (Supplemental Fig. 11), suggesting that the ectopic TdT+ GMPs are not differentially susceptible to apoptotic cell death and may simply differentiate into more mature myeloid cells. To test this hypothesis, we flow sorted the CFU-E, Pre-CFU-E and Pre-MegE from control and *Lsd1*-CKO BM and then seeded all three erythroid progenitor populations as a mixture into MethoCult semi-solid media to test their differentiation potential (Fig. 4D). The majority of these erythroid progenitors in the control mice gave rise to BFU-E, Meg and MegE colonies as well as very few GM colonies (possibly contaminants contributed by slight gating differences during cell sorting). In contrast, erythroid progenitors from *Lsd1*-CKO mice largely shifted differentiation potential from BFU-E to GM lineages, as the majority of colonies generated from *Lsd1* CKO erythroid progenitors acquired GM characteristics (Fig. 4E). To determine whether the CFU-GM colonies derived from *Lsd1* CKO erythroid progenitors are indeed myeloid cells, we picked individual colonies from *Lsd1* CKO-seeded media and subjected the cells to flow cytometry, examining cell surface markers Gr1, CD11b and Ter119. The majority of these individual GM colonies were composed of cells that were Gr1+ or CD11b+; most significantly, none of the cells expressed the erythroid lineage Ter119+ marker (Fig. 4F), indicating that these

myeloid colonies arose from early erythroid (CFU-E or Pre-CFU-E) progenitors in Tx-treated *Lsd1* CKO mice.

To test the hypothesis that LSD1 inhibition leads to an erythroid to myeloid cell fate switch (EMS) using an orthogonal strategy, we next isolated untreated CFU-E, Pre-CFU-E and Pre-MegE from wild type mice by cell sorting. The cells were treated with either DMSO or increasing concentrations of LSD1i in the MethoCult semi-solid media. Consistent with the data from genetic *Lsd1* LOF (Fig. 4E), LSD1i treatment of these cultures induces EMS in a dose-dependent manner (Fig. 4G). Notably, 3 μM LSD1i treatment completely switches the erythroid to a myeloid lineage progenitor differentiation potential. Taken together, these data strongly support the hypothesis that both *Lsd1* genetic LOF or LSD1 pharmacological inhibition in erythroid progenitor cells leads to an erythroid to myeloid cell fate conversion.

Pu.1 **is activated at the CFU-E stage in** ***Lsd1*** **CKO mice**

To better understand the molecular basis for why *Lsd1* LOF in erythroid progenitors leads to gain-of GMP features, we flow sorted CFU-E cells from *Lsd1* CKO and control mice (Fig. 3D). When we compared gene expression profiles in the two populations, LSD1 mRNA was reduced (as anticipated) by more than 90% in the CKO cells. PU.1 is a well characterized transcription factor that is critical for myeloid differentiation[52-54], and transcriptional activation of *Pu.1* is regulated by RUNX1 in HSPC[55]. Consistent with the observed increase in GMP activity in *Lsd1* CKO mice, PU.1 expression levels were 7-fold higher in CFU-E recovered from their bone marrow. In the same cells, GATA1 mRNA was slightly but significantly reduced, another indication of impaired erythroid differentiation, whereas RUNX1 levels were unchanged (Fig. 5A).

Erythroid LSD1 inhibition activates ectopic ***Pu.1*** **expression**

To further explore whether LSD1 inhibition in erythroid progenitor cells de-represses the expression of common myeloid markers, we performed qRT-PCR on human CD34+ cell-derived erythroid cells after 14 days of *in vitro* differentiation culture in the absence or

presence of either TCP or CCG50 LSD1 inhibitors (Supplemental Fig. 1B). Consistent with the *in vivo* data, both inhibitors significantly activated two myeloid regulatory genes, *Pu.1* and *Cebpa*, whereas expression of the key erythroid regulator GATA1 was significantly impaired (Fig. 5B). Notably, treatment with either LSD1 inhibitor also significantly induced RUNX1 expression *in vitro* (Fig. 5B) even though *Lsd1* genetic LOF does not affect *in vivo* RUNX1 expression in murine CFU-E (Fig. 5A).

To test whether LSD1 directly regulates *Pu.1* expression, we performed LSD1 ChIP assays in HUDEP2 cells, a human cell line that most closely corresponds to human adult definitive erythroid cells[56]. The results show that LSD1 is bound at the transcriptional start site of the human *Pu.1* gene (Fig. 5C), an observation consistent with LSD1 ChIP-seq data reported for K562 myeloerythroid lineage cells (UCSC genome browser).

To determine whether LSD1i also induces EMS in primary human CD34+ cells, we performed flow cytometry at d11 of erythroid differentiation after four days of LSD1i or vehicle (DMSO) treatment (Supplemental Fig. 1B). LSD1i addition enhanced expression of myeloid cell surface marker CD11b in these erythroid differentiation cultures, up to 4.1% of total, in a dose dependent manner (Fig. 5D). The efficiency of EMS in the CD34+ cell differentiation cultures was less pronounced than in semi-solid culture media (Fig. 4E-G), perhaps as a consequence of missing myeloid cytokines in the erythroid differentiation media.

In summary, these data indicate that LSD1 normally acts to repress *Pu.1* expression in order to maintain erythroid lineage potential in hematopoietic progenitor stages. Once *Lsd1* is deleted or LSD1 protein is inactivated by chemical inhibitors, *Pu.1* is induced in erythroid progenitors, likely through increased activity of RUNX1[55], which initiates the GMP cascade and impairs normal erythroid differentiation (Fig. 5E).

***Pu.1* or *Runx1* LOF rescues the LSD1i-mediated block in erythroid differentiation**

To test whether or not the RUNX1/PU.1 axis plays a functional role in blocking erythroid differentiation that is induced by LSD1 genetic or pharmacological inactivation, we generated

Pu.1 or *Runx1* homozygous knockout HUDEP2 cell clones to ask whether ablation of either gene could rescue the erythroid differentiation blocking effects of LSD1 inhibition. For each gene, four clones were generated using two different sgRNAs. Properly targeted mutation of all clones (except one) was confirmed by Sanger sequencing (Supplemental Figs. 12, 13). Three different non-targeting sgRNAs (NT1, NT4 and NT3) containing scrambled guide sequences were used to generate negative control HUDEP2 clones.

LSD1i treatment at 300 nM significantly reduced the erythroid fractional percentage of CD71+CD235a+ cells (by 50%) in control HUDEP2 cells (Fig. 6A and Supplemental Figs. 14A, 14B), further confirming that LSD1i treatment impairs erythroid differentiation. The percentage reduction in CD71+CD235a+ cells was rescued by either *Pu.1* or *Runx1* knockout (Fig. 6A and Supplemental Fig. 14). Consistent with the erythroid differentiation block visualized by flow cytometry, LSD1i treatment of control HUDEP2 cells repressed γ-globin, β-globin and GATA1 expression, and activated *Pu.1* expression, effects which could be rescued in *Pu.1* or *Runx1* knockout HUDEP2 cell clones (Fig. 6B). Taken together, the data indicate that RUNX1/PU.1 activation plays a key role in blocking erythroid lineage differentiation that is induced by LSD1 inhibition.

RUNX1 inhibitor treatment rescues the LSD1i-mediated block in erythroid differentiation

As LSD1 inhibitors have been proposed as potential therapeutic agents for SCD clinical treatment, we next ask if pharmacological inhibition of the RUNX1/PU.1 pathway could rescue the erythroid differentiation blocking effects of LSD1 inhibitor treatment. As no effective PU.1 inhibitor is commercially available, we tested Ro5-3335, a published RUNX1 inhibitor (RUNX1i) [57]. To investigate whether co-treatment with a genuine and well charcterized RUNX1i plus LSD1i could rescue the erythroid differentiation defect caused by LSD1i treatment, we also added RUNX1i AI-10-104[58] to the CD34+ erythroid differentiation cultures.

Either RUNX1i was added to CD34+ erythroid differentiation media at the same time as LSD1i, and erythroid cell maturation was examined at d11 by flow cytometry (Supplemental Fig. 1C). Treatment with either LSD1i alone inhibited erythroid differentiation as indicated by the reduced production of CD71+CD235a+ cells (Fig. 7A). However, co-treatment of cultures with either LSD1i plus RUNX1i rescued the erythroid differentiation block in a dose dependent manner (Fig. 7A). Although RUNX1i co-treatment rescued the erythroid differentiation block induced by LSD1i, significant cell death was also observed at d11 after Ro5-3335 addition (data not shown). To exclude the effect of RUNX1i-induced cell death during erythroid differentiation, we analyzed cells at d9, just two days after treatment with LSD1i, RUNX1i or both (Supplemental Fig. 15A). We found that co-treatment with either RUNX1 inhibitor partially rescued the LSD1i-mediated erythroid differentiation block (Fig. S15B).

Finally, we examined γ- and β-globin expression after treating the CD34+ erythroid differentiation cultures with RUNX1i, LSD1i or both, at d11 (Fig. 7B). RUNX1i co-treatment with LSD1i significantly rescued globin gene expression that was repressed by LSD1i treatment alone. Surprisingly, γ-globin expression was induced 4-fold by RUNX1i treatment alone, suggesting that RUNX1 may play a previously uncharacterized but LSD1-independent role in fetal globin gene repression in adult erythroid cells (Fig. 7B). Taken together, the data show that pharmacological inhibition of the RUNX1/PU.1 axis partially rescues the differentiation block induced by LSD1i treatment of erythroid precursor cells.

Discussion

In this study, we set out to investigate the effects of LSD1 inhibition on erythropoiesis *in vivo*; this required the generation of an erythroid lineage-specific, inducible Cre deleter line to investigate the effects of conditional *Lsd1* loss-of-function in murine adult definitive erythroid cells. Previously, Takai *et al*. showed that a 196 kb mouse *Gata1*-GFP knock-in BAC exhibited prominent GFP expression in MEP and that this fluorescence continued to peak as erythropoiesis (at the CFU-E and proerythroblast stages) progressed, and then gradually weakened in basophilic and polychromatic erythroblasts[43]. Interestingly, they also reported that the first (weak) hematopoietic GFP fluorescence was detected in CMP; however, in *R26T:G1B*CreER^{T2} mice that were treated with tamoxifen, no CMP cells labeled with TdTomato. This could be due to the abundance of the CreERT2 fusion protein in CMP of *G1B*CreER^{T2} mice that somehow does not approach a threshold required for efficient loxP recombination, thus coincidentally causing the *G1B*CreER^{T2} transgene to be highly erythroid-specific. In the *R26T:G1B*CreER^{T2} mice, we observed that about 5% of Tx-treated LSK cells were labeled by TdTomato. However, none of the downstream myeloid progeny (such as GMP) were TdTomato+, indicating that the GATA1+ LSK cells in these mice do not differentiate into myeloid lineage cells.

Here we report that the loss of LSD1 activity either *via* pharmacological inhibition in human CD34+ HSPC or through genetic deletion in mice leads to disrupted adult erythropoiesis. In human erythroid HSPC differentiation cultures, a novel LSD1 inhibitor (CCG50) blocks erythropoiesis in a dose-dependent manner during the early stages of culture (from days 7 to 11) when hSCF is included in the culture media. After withdrawal of hSCF, erythroid differentiation temporarily recovers (fully or partially, depending on inhibitor concentration) by day 14, suggesting that the first effect of LSD1 inhibition is hSCF-dependent, which very likely occurs during progenitor cell stages. Furthermore, the production of reticulocytes is impaired, indicating that a second effect of LSD1 inhibition occurs at a late erythroid maturation stage. In agreement with the latter hypothesis, we also

observed deficiencies at both the erythroid progenitor and late erythroblast stages in the *Lsd1* conditional loss-of-function mice. Global transcriptomic analyses of the affected cell stages may provide additional molecular mechanistic insights into how loss of LSD1 affects erythroid differentiation and clues for how to eliminate or minimize any toxic effects of LSD1 inhibition in the future.

The *in vivo* role of LSD1 within the murine hematopoietic compartment has been explored previously. Using the pan-hematopoietic Mx1Cre transgene to facilitate conditional inactivation of *Lsd1,* Kerenyi *et al.* reported that LSD1 deficiency impacted HSC self renewal[33]. Furthermore, they showed that EpoRCre-mediated *Lsd1* deletion *in vivo* resulted in prenatal lethality due to anemia. Using the newly generated *G1B*CreER^{T2} deleter line reported here, we were able to examine the consequences of LSD1 ablation in adult erythropoiesis for the first time. We found that definitive erythropoiesis was compromised as a consequence of drastically reduced erythroid progenitor and precursor cell numbers.

GATA1 was previously reported to transcriptionally repress PU.1 expression by directly binding to GATA consensus sites at the TSS of *Pu.1* in erythroblasts[59]. We confirmed LSD1 binding at these same sites in the human erythroid HUDEP2 cell line by ChIP assays (Fig. 5C). It has been reported that a GATA2/TAL1/LSD1 complex binds to GATA sites to repress GATA1 transcription during erythroid differentiation[60]. Similarly, perhaps a GATA1/LSD1 complex may cooperatively repress *Pu.1* transcription in erythroid cells. Interestingly, PU.1 forced overexpression impairs erythroid differentiation and leads to erythroleukemia in mice[61]. Mice that express GATA1 at 5% of wild type levels display a propensity for erythroleukemia[47]. Curiously, we detected the expansion of a GMP-like population as well as a new population that was immunophenotyped as Lin-cKit+Sca1-CD34-CD16/32+ in LSD1 erythroid-restricted knockout mice (Fig. 4A). Whether these unusual cells might represent harbingers of a pre-leukemic state or a previously undiscovered myeloid progenitor state will required further investigation. In this regard, long term monitoring of possible leukemogenesis in the *Lsd1* CKO mice will certainly be interesting to investigate further.

Increased levels of LSD1 have been detected in different neoplasms, and LSD1 was shown to play a key role in carcinogenesis, highlighting the potential therapeutic effect of LSD1 inhibitors in cancer and myelodysplastic syndrome treatment[62]. However, LSD1 inhibitors have multiple side effects, thus potentially lessening their utility for targeted therapeutic development. One phase-I clinical study of LSD1 inhibitor TCP to treat AML and MDS patients showed that 13% of the patients developed anemia[63], a profound negative effect of this earliest LSD1 inhibitor that was originally applied to treat neurological disorders.

In this regard, the mechanisms of LSD1 action revealed in this study may illuminate a path to further development of safe and effective therapeutics for the treatment of the β-globinopathies, SCD and β-thalassaemia. From the data presented here, one could envision a safe and effective binary therapeutic compound that both induces fetal hemoglobin (by blocking LSD1 activity) and at the same time promotes normal erythroid differentiation by blocking the induction of PU.1 and/or RUNX1 in HSPC. The identical treatment could be equally applicable to the treatment of AML and/or MDS patients suffering from malignant or pre-malignant neoplasms.

Materials and Methods

Erythroid differentiation of human CD34+ cells. Human CD34+ HSPCs from healthy donors were purchased from Fred Hutchinson Cancer Research Center. The CD34+ cells were cultured and differentiated into mature erythroid cells using a standard three-phase culture system[36]. The basic media was composed of Iscove's Modified Dulbecco's Medium (IMDM) supplemented with 5% pooled human AB plasma (Octaplas, Rhode Island Blood Center), 1x penicillin-streptomycin (Gibco), 1% L-glutamine, 330 µg/ml holo-transferrin (T4132, Sigma), 2 IU/ml heparin (H3149, Sigma), and 10 μg/ml human insulin (91077C, Sigma).

From day (d) 0-7 of the expansion culture period, the basic medium was supplemented with 1 μM hydrocortisone (07904, Stem Cell Technologies), 5 ng/ml human IL-3 (203-IL, R&D), 100 ng/ml human SCF (255-SC-050, R&D), and 3 IU/ml erythropoietin (Epoetin Alfa, Amgen). Hydrocortisone and IL-3 were withdrawn from the media beginning on d8 while SCF was omitted after d12. On differentiation day (d) 7, CD34+ HSPC-derived erythroid cells were counted and reseeded at 10^5 cells/ml in the presence of increasing concentrations of LSD1i (0, 120 nM, 370 nM or 1.1 □M) for an additional 11 days.

The novel LSD1 inhibitor described in this manuscript (CCG50; LSD1i) was designed, synthesized and characterized by the Center for Chemical Genomics at the University of Michigan, and will be described in a separate study (in preparation). At d7 of erythroid differentiation, cells (10^5/ml) were cultured in the presence of DMSO or 3-fold dilutions of LSD1i (1.1 μM, 370 nM or 120 nM; Fig. S1B). Thereafter, the medium was changed at d11 and d14 with freshly added LSD1i. At the indicated time points, aliquots of cells were removed for flow cytometric, RNA and/or HPLC analyses. Experiments were repeated using CD34+ cells from at least two separate donors.

***In vitro* LSD1 inhibition assay.** A fluorescent *in vitro* LSD1 inhibition assay (Item No. 700120, Cayman Chemicals) was performed according to the manufacturer's instructions.

HPLC. On the day erythroid differentiation terminated, cells were washed with PBS and the cell pellets were lysed; the contents were then subjected to HPLC analyses using a BioRad CDM System CDM5.1 VII Instrument according to the manufacturer's instructions.

Total RNA isolation and qRT-PCR analyses. Total RNA was isolated from cells using Trizol (ThermoFisher Scientific) or RNeasy Micro Kit (Qiagen) according to manufacturer's instructions. cDNA was synthesized using SuperScript III Reverse Transcriptase (ThermoFisher Scientific). qRT-PCR was performed using FastSybr Green Mastermix on an ABI Step One Plus instrument (ThermoFisher Scientific). Sequences of all primers are listed in Supplementary Table 1.

BAC recombination. BAC recombination and the 196 kbp mouse *Gata1* BAC clone (RP23-443E19) have been described previously[43,64]. Briefly, the targeting DNA fragment was constructed by inserting a CreERT2-polyA-Neo cassette at the translational start site of mouse *Gata1* (in the 2nd exon) between 5' and 3' homologous recombination arms. The resultant targeting DNA fragment was excised from the cloning vector and transfected into transiently heat-activated EL250 bacteria (to induce recombinase expression) containing BAC RP23-443E19. Recombinant bacterial colonies (with newly acquired Kanamycin resistance) were individually screened for homologous recombination at the *Gata1* ATG by PCR using two primer sets (Supplemental Table 1). Clones that were determined to have successfully recombined (CreER^{T2} Neo+) were then cultured in the presence of L-arabinose to induce flp recombinase expression to promote excision of the frt-flanked Neo selection marker. Finally, the BAC DNA was purified by NucleoBond BAC100 and submitted for microinjection into fertilized egg of C57BL6 background mice (Transgenic Animal Model core, University of Michigan). Primers are listed in Supplementary Table 1.

Mice. *G1B*CreER^{T2} transgenic founders were intercrossed with wild type C57BL6 mice for three generations to eliminate possible mosacism and to confirm germline transmission. Two lines, L245 and L259, were interbred with Cre reporter mice R26 tdTomato [45] (Jackson Stock# 007914) or homozygous *Lsd1*$^{f/f}$ mutant mice[50]. To induce *G1B*CreER^{T2} activity, mice (from 8-12 weeks old) were injected intraperitoneally with tamoxifen (Tx; 2 mg per injection on alternate days for 2 weeks). All animal procedures were approved by the Institutional Animal Care and Use Committee of the University of Michigan (IUCAC Protocol PRO00009778). Primer sequence for genotyping are listed in Supplemental Table 1.

Differential peripheral blood analyses. Peripheral blood was collected from mice by facial vein bleed into EDTA-treated tubes and analyzed on a Hemavet according to the manufacturer's instructions.

Genomic DNA qPCR. Genomic DNAs were purified from FACS-sorted mouse basophilic erythroblasts. To quantify *Lsd1* deletion efficiency, qPCR was performed using FastSybr Green Mastermix (Applied Biosystems) and *Lsd1* primer pairs that specifically annealed to genomic sequences within (P1) or outside of (P2) the two LoxP sites flanking *Lsd1* exon 6 [50](Fig. 3H). Deletion efficiency was calculated from the Ct ratio of P1/P2 as described previously[50,65]. The primers used for qPCR analysis are listed in Supplemental Table 1.

Flow cytometry. Total bone marrow (BM) isolation and subsequent antibody staining protocols were described previously[66]. AnnexinV staining was performed as described previously [41]. Flow analysis was performed on a BD Fortessa while flow sorting was performed on a BD Aria III. Antibodies used for flow cytometry are listed in Supplemental Table 2.

ChIP. ChIP assays were conducted as described previously[26].

Colony-Forming Unit (CFU) assay. Isolated total BM cells or purified, sorted cell populations were counted and seeded into Methocult M3434 or M3334 (Stemcell Technologies) according to manufacturer's instructions for enumeration of BFU-E, CFU-GM, CFU-GEMM or CFU-E colonies.

CRISPR knockout of *Pu.1* or *Runx1* genes. Genome edited *Pu.1* or *Runx1* loss of function strategy was essentially as described in a previous study[26]. Individual HUDEP2 *Pu.1* or *Runx1* targeted clones were initially identified by PCR (sequences shown in Supplemental Table 1) and verified by Sanger sequencing. One clone (P2-4) exhibited no amplification of the guide-targeted exon, suggesting that this clone bore a large genomic DNA deletion (data not shown). The guide sequences used for gene editing are also listed in supplemental Table 1.

Acknowledgements

We gratefully acknowledge the assistance and insights provided by multiple colleagues at the University of Michigan (Sojin An, Uhnsoo Cho, Susan Hagen, Pil Li and Mathivanan Packiarajan). We gratefully acknowledge continued support from the NHLBI (awards U01 HL117658 and P01 HL146372; JDE and AW), from the Cooley's Anemia Foundation (LY) as well as a center of excellence award from the NIDDK (U54 DK106829) to the Fred Hutchinson Cancer Center to support the isolation and distribution of normal human hematopoietic stem and progenitor (CD34+) cells for the scientific community.

Figure legends

Figure 1: LSD1 inhibition activates fetal □-globin transcription but blocks erythroid differentiation. (A) Representative flow cytometry plots of human CD34+ HSPC cells undergoing erythroid differentiation after 11, 14 and 18 days (d) in culture. Cells were treated with DMSO or with 1.1μM, 370 nM or 120 nM LSD1 inhibitor CCG050. Cells were monitored for CD71 and CD235a cell surface markers whose acquisition reflect maturing erythroid differentiation stages[37]. Numbers in each quadrant indicates the percentage of gated cells. Results are representative of experiments performed using CD34+ HSPCs from two different healthy adult donors. (B) Representative HPLC chromatograms of d18 cells cultured with or without CCG050 from (A). HbF percentage at each inhibitor concentration is indicated in parentheses. (C) The percentage of γ-globin transcripts in total β-like (γ+β) globin mRNAs at d14. (D) mRNA abundance of γ-globin and β-globin (normalized to OAZ1 internal control mRNA)[26] at d14. The γ-globin transcript abundance in DMSO-treated cells was arbitrarily set at 1. (E) Transcript levels of key erythroid transcription factors GATA1, KLF1 and TAL1 (normalized to OAZ1 mRNA) were reduced in d14 cells treated with 370 nM LSD1 inhibitor CCG050. Transcript levels of each mRNA in DMSO-treated cells were arbitrarily set at 1. Data are shown as the means ± SD from three replicates (*** $p<0.001$; unpaired Student's t-test).

Figure 2: Inducible, erythroid-specific *G1B*CreER^{T2} expression is initiated at the MEP stage. (A) Representative flow cytometry plots showing gating strategies for the anti-CD71 and -Ter119 antibodies used to identify progressively more mature erythroid cells (from stages II to V) among BM cells of untreated (left panel) or 2 mg of Tx (2 mg for 5 times every other day; right panel) -treated *R26T*:*G1B*CreER^{T2} line 259 mice. (B) Representative flow histograms showing TdTomato epifluorescence in cell fractions I-V (as gated in A.) from DMSO-treated (blue peaks) or Tx-treated (red peaks) *R26T*:*G1B*CreER^{T2} murine transgenic lines L245 (top) or L259 (bottom) bone marrow cells. (C) Representative flow histograms

showing TdTomato epifluorescence in the BM Lin-cKit+Sca1+ (LSK), CMP (Lin-cKit+Sca1-CD34+CD16/32-), GMP (Lin-cKit+Sca1-CD34+CD16/32+), MEP (Lin-cKit+Sca1-CD34-CD16/32-) and CFU-E (Lin-cKit+Sca1-CD16/32-CD41-CD150-CD105+) populations (more detailed gating strategies are shown in Supplemental Figs. 5, 6) in untreated (blue peaks) or Tx-treated (red peaks) *R26T*:*G1B*CreER^{T2} (line 259) cells.

Figure 3: Effects of *Lsd1* deletion in erythroid cells of conditional knockout mice. *Lsd1* CKO and control mice were administered seven Tx IP injections on alternate days. Total BM cells were harvested and processed for colony assays and flow cytometric analyses. (A) Colony numbers of CFU-GEMM, CFU-GM, BFU-E and CFU-E per 10^5 BM cells of control and *Lsd1* CKO mice. (B) Representative micrographs of BFU-Es from control or *Lsd1* CKO mice taken at low or high (inset) magnification on day 10 of CFU assay. Scale bar = 200 μM. (C) No statistically significant difference is observed in the spleens (as percentages of body weights) of control versus *Lsd1* CKO mice. (D) Representative flow cytometry plots displaying the gating for CFU-Es of control and *Lsd1* CKO mice. (E) Bar graph showing absolute numbers of CFU-E in control and *Lsd1* CKO mice (per two femurs + two tibias). (F) Representative flow cytometric plots showing the gating strategy for defining CD71+Ter119+ erythroid precursor cells (top panels), which were subsequently gated by CD44 staining versus forward scatter (FSC) to separate basophilic erythroblasts (BasoE), polychromatic erythroblasts (PolyE) and orthochromatic erythroblasts (OrthoE)[bottom panels]. (G) Absolute numbers of BasoE, PolyE and OrthoE in control and *Lsd1* CKO BM. (H) Deletion efficiency of *Lsd1* flox alleles in flow-sorted BasoE was determined by qPCR. Primer pair P1 detects *Lsd1* genomic DNA flanked by the two loxP sites while primer pair P2 detects *Lsd1* genomic DNA that is unaffected by Cre-mediated deletion. Data are shown as the means ± SD. (*** $p<0.001$; unpaired Student's t-test).

Figure 4: LSD1 LOF shifts erythroid differentiation potential to the GM lineage. Representative flow cytometry plots showing the gating strategies for Lin-Sca1+cKit+ (LSK)

cells, CMP, GMP and MEP (A), and their absolute cell numbers (B) in Tx-treated *Lsd1* CKO or control mouse BMs. (C) TdTomato epifluorescence was analyzed in individual cell populations of Tx-treated R26T:*G1B*CreER^{T2} control (blue peaks) or *Lsd1* CKOT (red peaks) mice. (D) Erythroid progenitors give rise to GM colonies in LSD1-CKO BM. Sorted CFU-E, Pre-CFU-E and Pre-MegE from Tx-treated control and *Lsd1* CKO mice were pooled for seeding in colony forming unit assays. Colony types [Meg, mixed MegE, GM and BFU-E (per 600-sorted cells)] were quantified and presented in panel (E) (F) Representative flow cytometry plots of individual GM colonies picked from the *Lsd1*-CKO. The cells were stained with anti-Gr1, -CD11b or -Ter119 antibodies. (G) Colony numbers of Meg, MegE, CFU-GM and BFU-E per 600 sorted cells of control mice treated with DMSO or different concentrations of CCG50 LSD1i. Data are shown as means ± SD from three mice. (** $p<0.01$; *** $p<0.001$; unpaired Student's t-test).

Figure 5: LSD1 directly inhibits myeloid differentiation genes in erythroid cells. (A) Relative mRNA levels of RUNX1, PU.1, LSD1 or GATA1 (normalized to 18s ribosome RNA) in sorted CFU-E cells from Tx-treated control and *Lsd1*-CKO mouse BM. (B) Histograms depicting the relative mRNA levels of human PU.1, CEBPα, RUNX1 and GATA1 (normalized to OAZ1 transcript level) in d14 erythroid cells differentiated from human CD34+ cells at d14 of culture assayed by qRT-PCR. Cells were expanded in the presence of DMSO or LSD1 inhibitors TCP (3 □M) or LSD1i (at three different concentrations). (C) ChIP-qPCR analysis of LSD1 binding to the PU.1 promoter in HUDEP2 cells. Differential enrichment was detected at the PU.1 transcriptional start site (TSS, black bar), but not at an adjacent site included as a negative control (gray bar). Rabbit IgG was included as a negative control. (D) CCG50 treatment enhances CD11b expression during erythroid differentiation induction of human CD34+ cells. Cells were treated with LSD1i (100 nM, 300 nM or 1 μM) or DMSO on day 7. CD11b and CD235a were analyzed at d11 of differentiation. Data are shown as the means ± SD. (* $p<0.05$; ** $p<0.01$; *** $p<0.001$; unpaired Student's t-test). (E) LSD1

maintains normal erythropoiesis by repressing Pu.1 expression in erythroid progenitors. LSD1 gene deletion or protein inhibition leads to abnormal activation of *Pu.1*, likely through RUNX1, and shifts the differentiation potential from the erythroid to myeloid lineage.

Figure 6. *Pu.1* or *Runx1* genetic knockout rescues the erythroid differentiation inhibition induced by blocking LSD1 activity. (A) CD71 and CD235a flow cytometric analysis of three independent non-targeting sgRNA infected cells (WT, left), four *Pu.1* -/- clones (middle) or four *Runx1*-/- clones (right) treated with DMSO (control) or 300 nM CCG50. Data are shown as the average value of percentage of CD71+CD235a+ cells from multiple clones in Supplemental Fig. 14. Impaired erythroid differentiation (as reflected by the reduced percentage of CD71+CD235a+ cells) in the WT group after CCG50 treatment was rescued by either *Pu.1* or *Runx1* knockout. (B) mRNA levels of γ-globin, β-globin, GATA1 or PU.1 in random sgRNA control cells after treatment with DMSO or 300 nM CCG50, or P3-18 (*Pu.1* -/-) and R2-47 (*Runx1*-/-) knockout clones treated with 300 nM CCG50. Data were shown as the means ± SD. (* $p<0.05$; ** $p<0.01$; *** $p<0.001$; unpaired Student's t-test).

Figure 7. RUNX1 inhibitor co-treatment partially rescues the erythroid to myeloid conversion by LSD1 inhibitors. (A) CD71/CD235a staining of human CD34+ cells showing erythroid differentiation at d11, after 4 days of treatment with CCG50 alone (300 nM or 1 μM), RUNX1 inhibitor Ro5-3335 alone (10 μM to 120 nM) or both. **(B)** mRNA abundance of γ-globin and β-globin at d11 after inhibitor treatments. γ-globin transcripts in DMSO were arbitrarily set at 1. Data is shown as the means ± SD. (* $p<0.05$; ** $p<0.01$; unpaired Student's t-test).

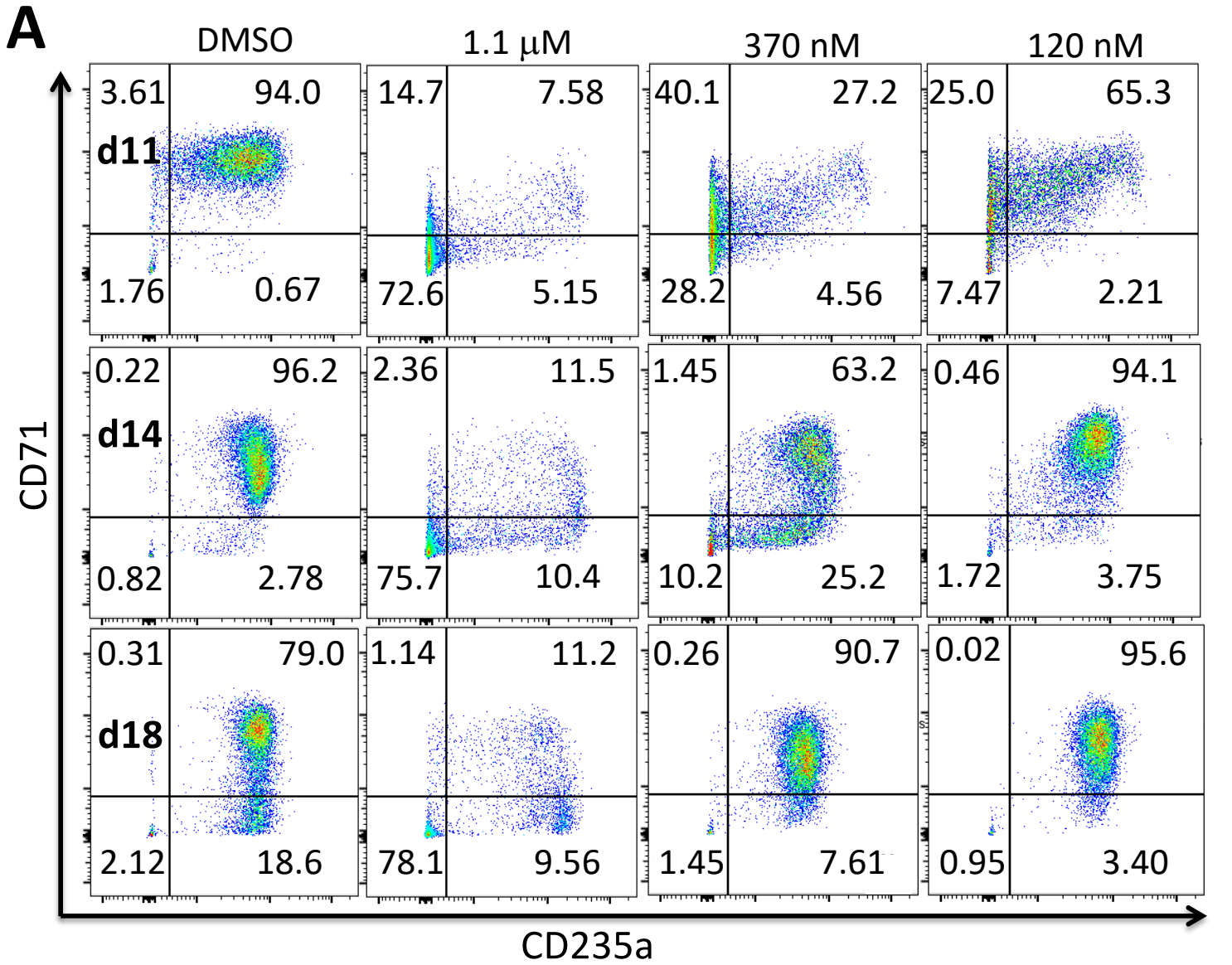
A
DMSO
1.1 μM
370 nM
120 nM
d11
3.61
94.0
1.76
0.67
14.7
7.58
72.6
5.15
40.1
27.2
28.2
4.56
25.0
65.3
7.47
2.21
d14
0.22
96.2
0.82
2.78
2.36
11.5
75.7
10.4
1.45
63.2
10.2
25.2
0.46
94.1
1.72
3.75
d18
0.31
79.0
2.12
18.6
1.14
11.2
78.1
9.56
0.26
90.7
1.45
7.61
0.02
95.6
0.95
3.40
CD71
CD235a

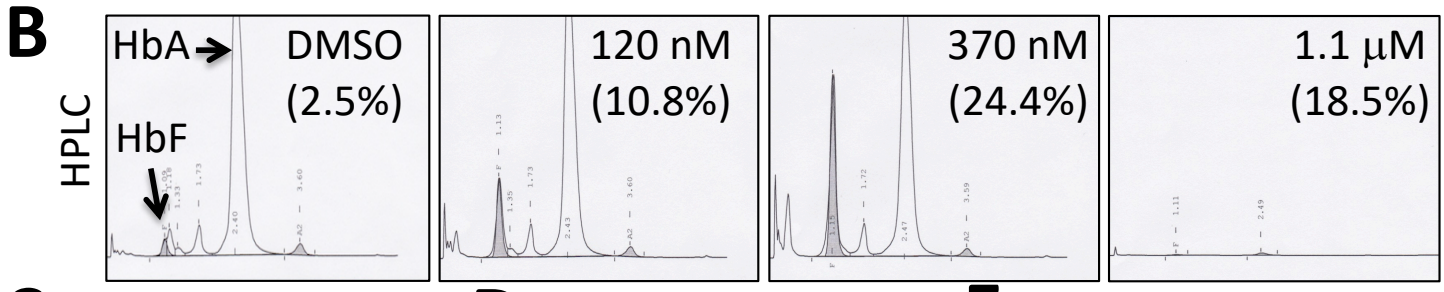
B
HPLC
HbA
HbF
DMSO
(2.5%)
120 nM
(10.8%)
370 nM
(24.4%)
1.1 μM
(18.5%)

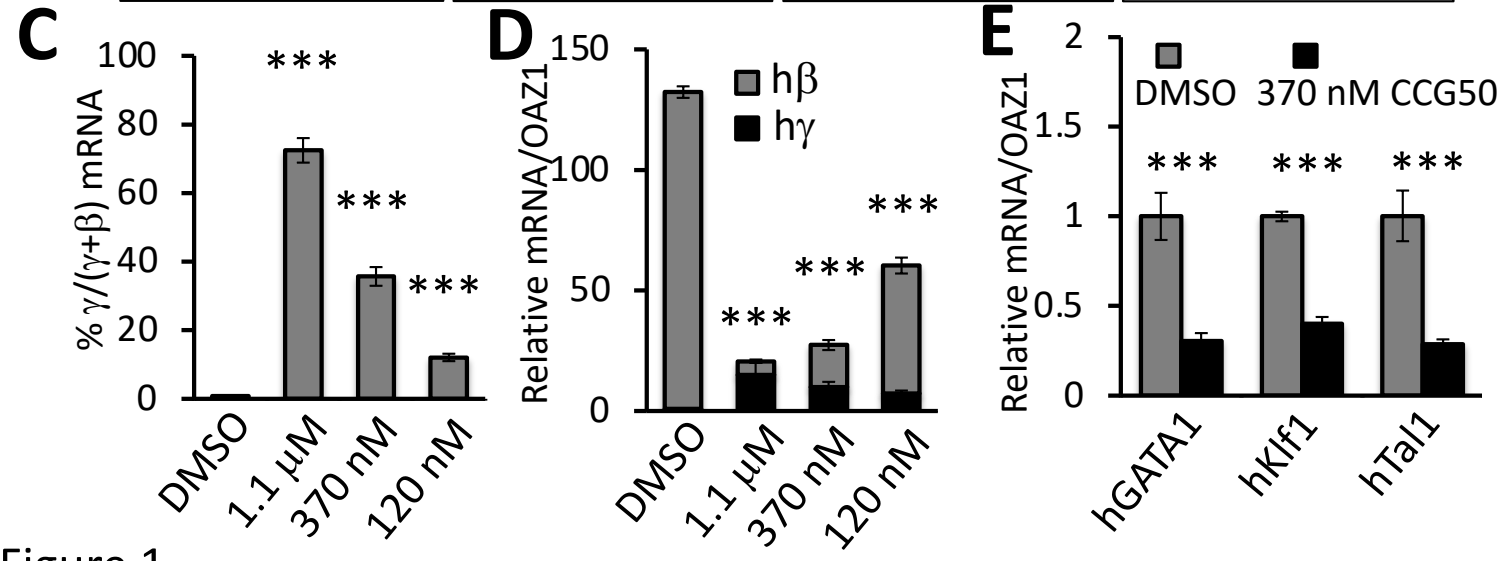
C
% γ/(γ+β) mRNA
100
80
60
40
20
0
***
***
***
DMSO
1.1 μM
370 nM
120 nM
D
Relative mRNA/OAZ1
150
100
50
0
hβ
hγ
***
***
***
DMSO
1.1 μM
370 nM
120 nM
E
Relative mRNA/OAZ1
2
1.5
1
0.5
0
DMSO
370 nM CCG50
***
***
***
hGATA1
hKlf1
hTal1

Figure 1

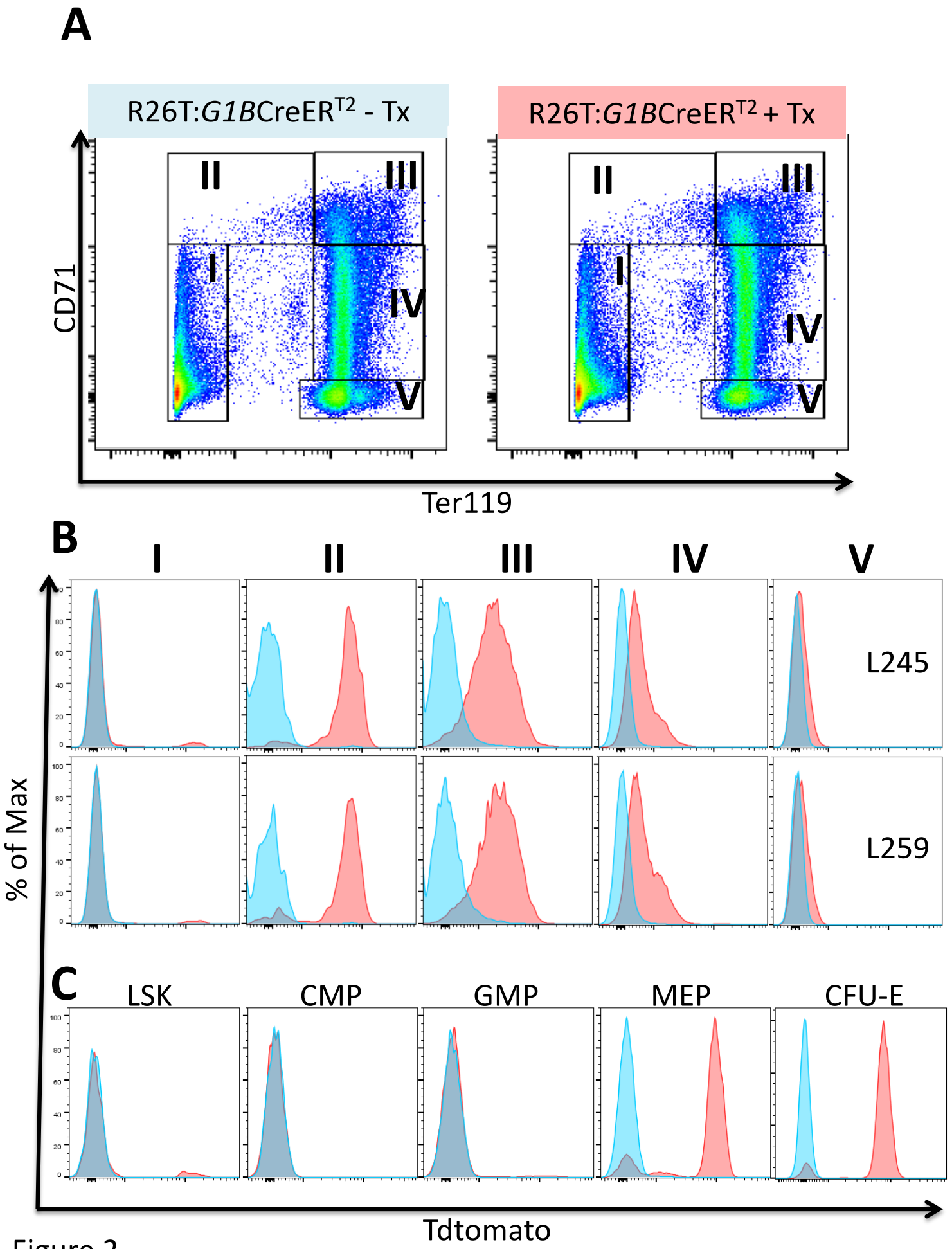
A
R26T:G1BCreER^{T2} - Tx
R26T:G1BCreER^{T2} + Tx
I
II
III
IV
V
CD71
Ter119
B
I
II
III
IV
V
L245
L259
% of Max
C
LSK
CMP
GMP
MEP
CFU-E
Tdtomato

Figure 2

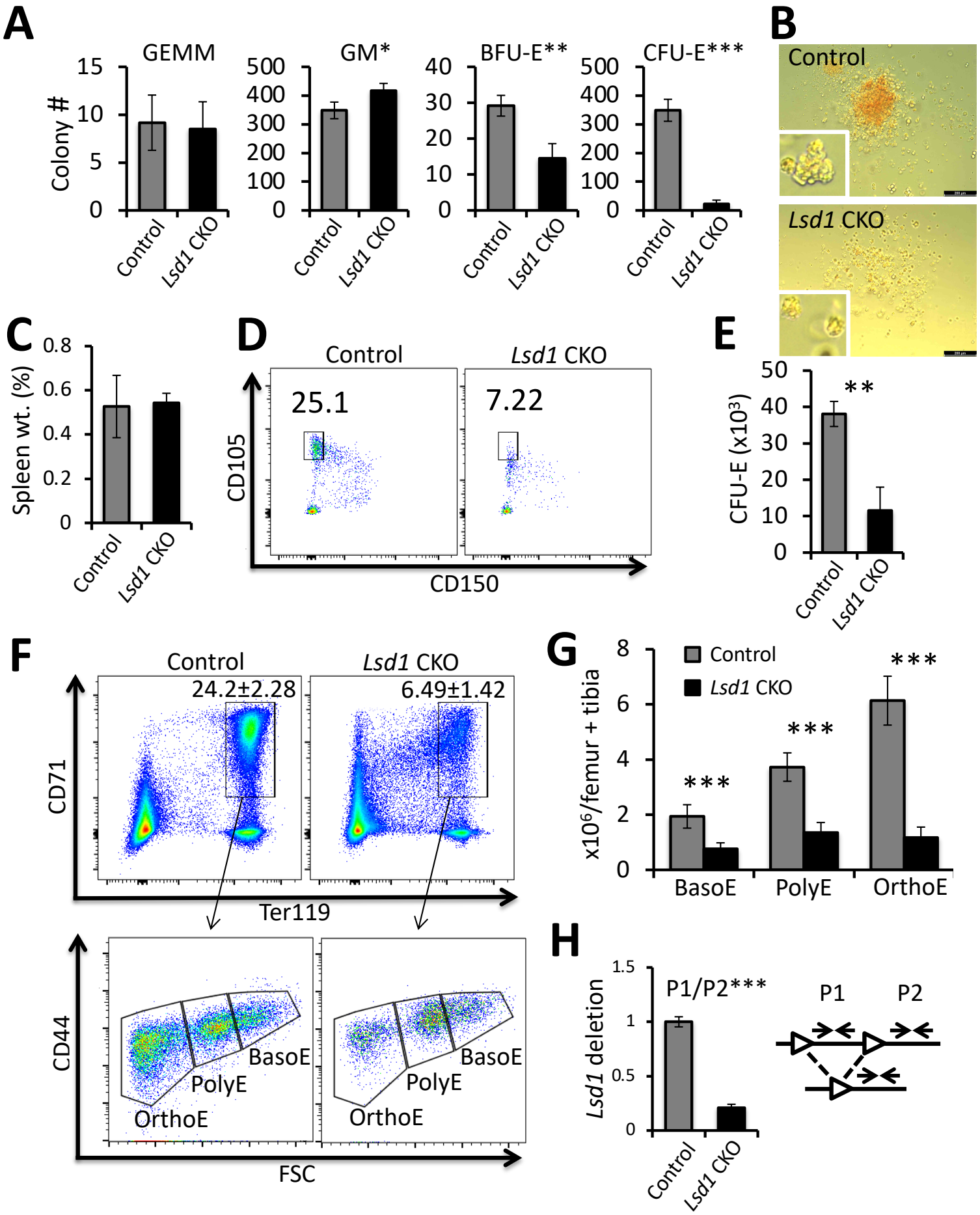
A
GEMM
GM*
BFU-E**
CFU-E***
Colony #
Control
Lsd1 CKO
B
Control
Lsd1 CKO
C
Spleen wt. (%)
D
Control
Lsd1 CKO
25.1
7.22
CD105
CD150
E
CFU-E (x10³)
**
F
Control
Lsd1 CKO
24.2±2.28
6.49±1.42
CD71
Ter119
CD44
FSC
BasoE
PolyE
OrthoE
G
x10⁶/femur + tibia
Control
Lsd1 CKO
***
BasoE
PolyE
OrthoE
H
Lsd1 deletion
P1/P2***
P1
P2

Figure 3

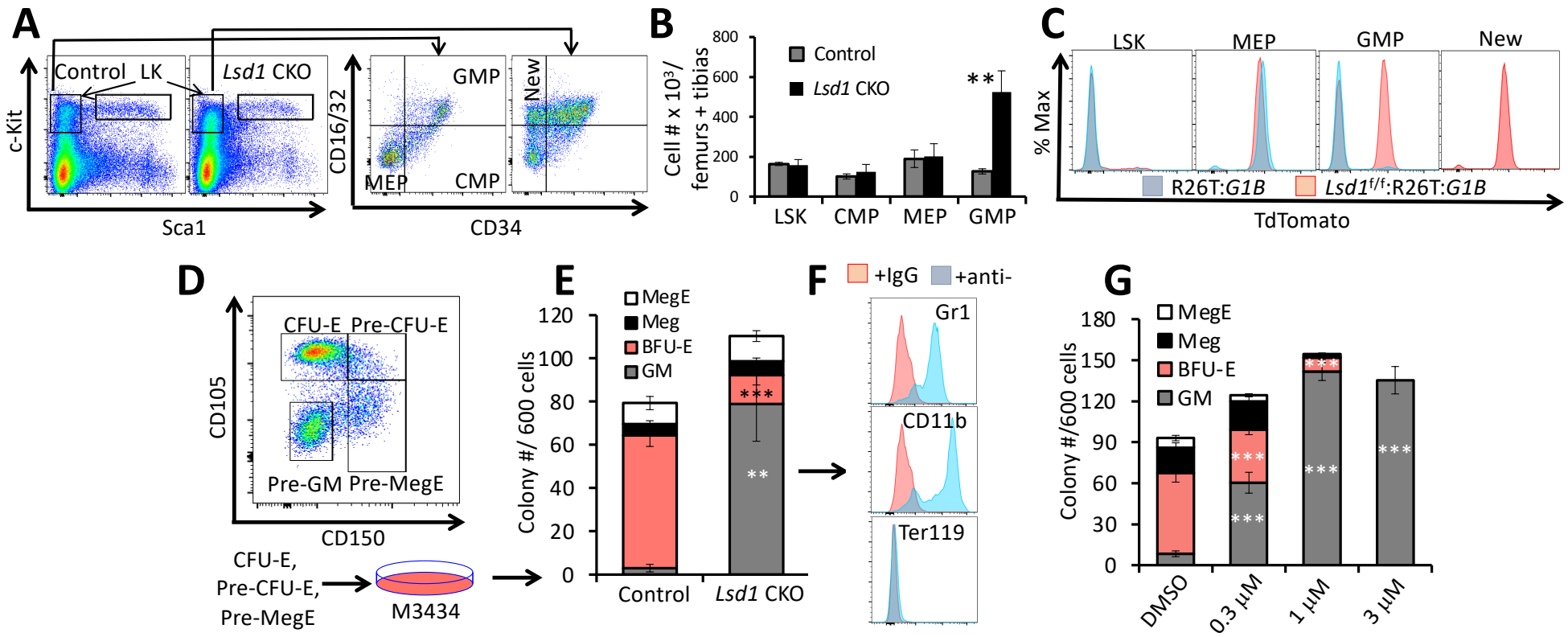
A
Control
LK
Lsd1 CKO
c-Kit
Sca1
CD16/32
GMP
New
MEP
CMP
CD34
B
Control
Lsd1 CKO
Cell # x 10³/ femurs + tibias
800
600
400
200
0
**
LSK
CMP
MEP
GMP
C
LSK
MEP
GMP
New
% Max
R26T:G1B
Lsd1f/f:R26T:G1B
TdTomato
D
CFU-E
Pre-CFU-E
Pre-GM
Pre-MegE
CD105
CD150
CFU-E,
Pre-CFU-E,
Pre-MegE
M3434
E
MegE
Meg
BFU-E
GM
Colony #/ 600 cells
120
100
80
60
40
20
0
***
**
Control
Lsd1 CKO
F
+IgG
+anti-
Gr1
CD11b
Ter119
G
MegE
Meg
BFU-E
GM
Colony #/600 cells
180
150
120
90
60
30
0
***
DMSO
0.3 μM
1 μM
3 μM

Fig4.

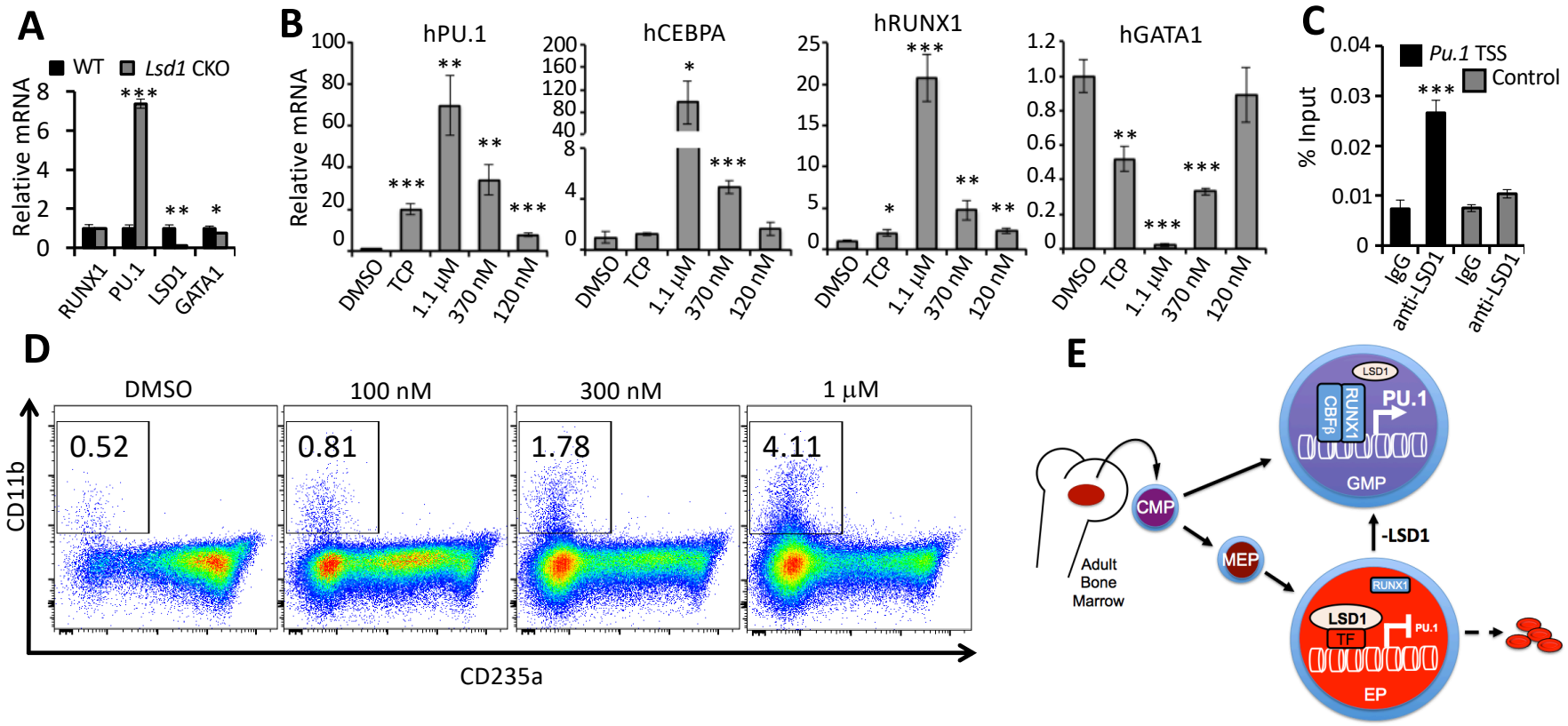
A
WT
Lsd1 CKO
Relative mRNA
RUNX1
PU.1
LSD1
GATA1
B
hPU.1
hCEBPA
hRUNX1
hGATA1
Relative mRNA
DMSO
TCP
1.1 μM
370 nM
120 nM
C
Pu.1 TSS
Control
% Input
IgG
anti-LSD1
D
DMSO
100 nM
300 nM
1 μM
0.52
0.81
1.78
4.11
CD11b
CD235a
E
Adult Bone Marrow
CMP
MEP
GMP
EP
LSD1
CBFβ
RUNX1
PU.1
TF
-LSD1

Fig5.

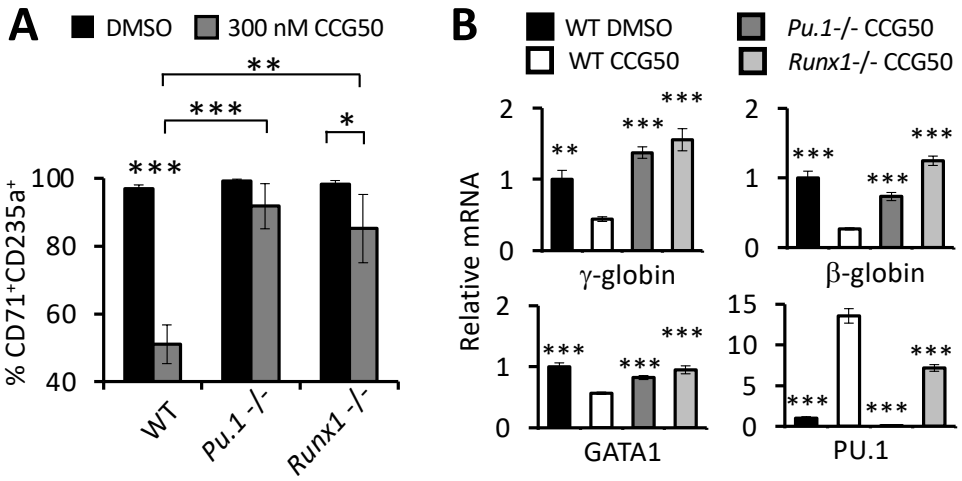
A
DMSO
300 nM CCG50
**
***
*
***
% CD71+CD235a+
100
80
60
40
WT
Pu.1 -/-
Runx1 -/-
B
WT DMSO
WT CCG50
Pu.1-/- CCG50
Runx1-/- CCG50
Relative mRNA
γ-globin
β-globin
GATA1
PU.1

Fig6.

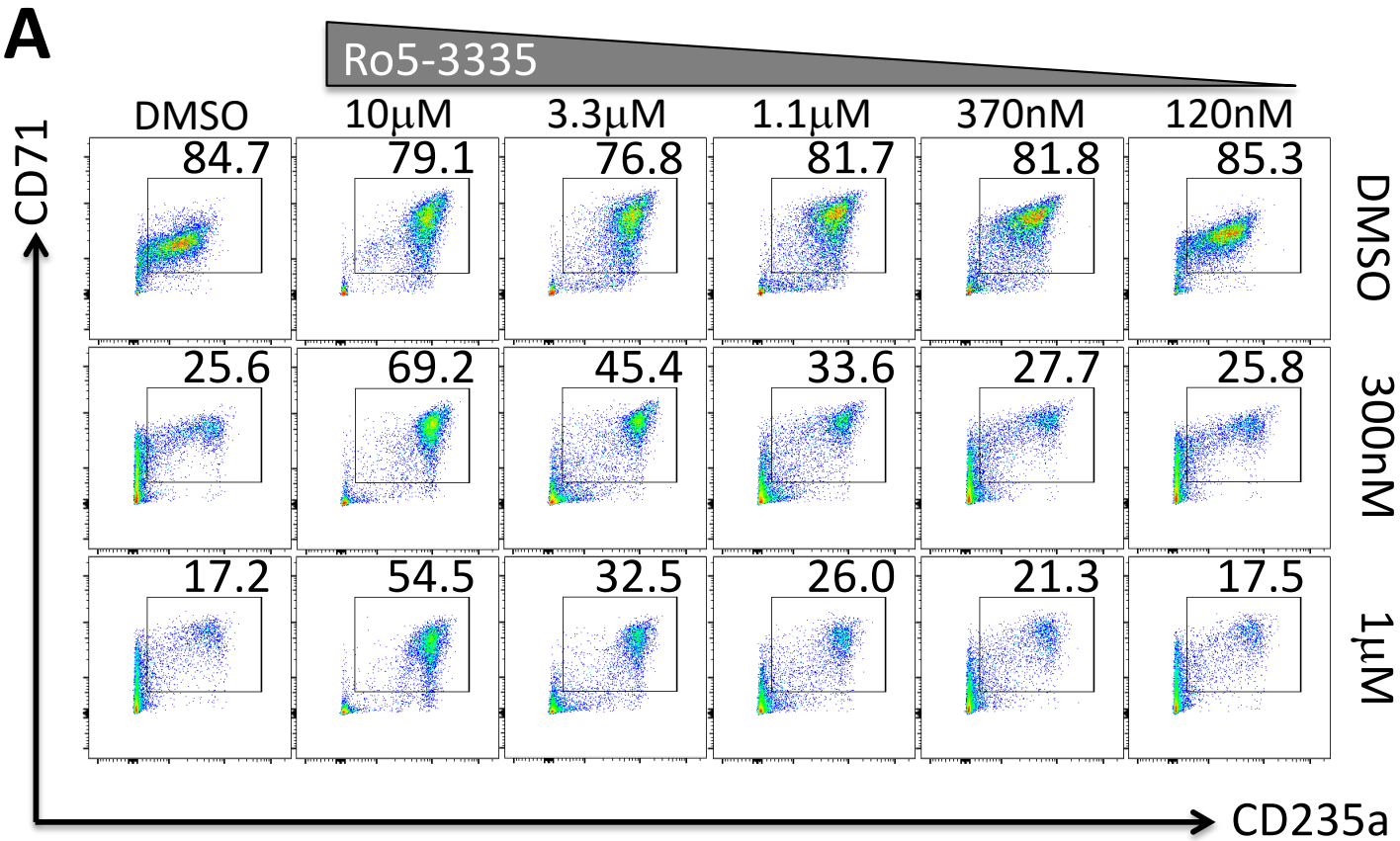
A
Ro5-3335
DMSO
10μM
3.3μM
1.1μM
370nM
120nM
CD71
84.7
79.1
76.8
81.7
81.8
85.3
DMSO
25.6
69.2
45.4
33.6
27.7
25.8
300nM
17.2
54.5
32.5
26.0
21.3
17.5
1μM
CD235a

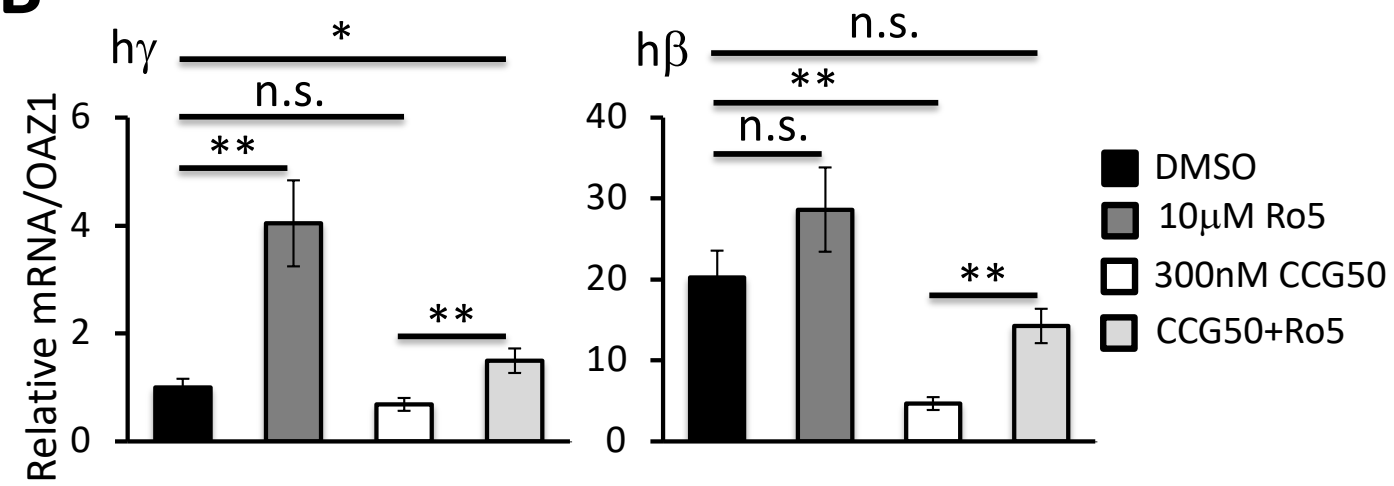
B
hγ
*
n.s.
**
**
Relative mRNA/OAZ1
6
4
2
0
hβ
n.s.
**
n.s.
**
40
30
20
10
0
DMSO
10μM Ro5
300nM CCG50
CCG50+Ro5

Figure 7

Table 1: Differential peripheral blood analysis of *Lsd1*-CKO mice and controls. Mice were IP injected with 2 mg of tamoxifen 7 times on alternate days prior to sacrifice. Data represent the counts of white blood cells (WBC); platelets (PLT); red blood cells (RBC); hemoglobin (Hb); hematocrit (HCT); mean corpuscular volume (MCV); mean corpuscular hemoglobin (MCH). Data are shown as the means ± SD from three to eight mice. (* $p<0.05$; ** $p<0.01$; *** $p<0.001$; unpaired Student's t-test).

	Control	*Lsd1*-CKO
WBC (x10^3/μl)	5.47±1.62	5.46±1.41
PLT (x10^3/μl)	785±125	1032±210*
RBC (x10^6/μl)	9.76±0.46	7.77±0.7**
Hb (g/dL)	12.67±0.4	9.66±0.67***
HCT (%)	43.4±2.71	31.12±2.15***
MCV (fL)	44.47±0.68	40.1±1.12***
MCH (pg)	13±0.26	12.42±0.43

Table 1

Literature Cited

1 Murayama, M. Molecular mechanism of red cell "sickling". *Science* **153**, 145-149, doi:10.1126/science.153.3732.145 (1966).

2 Platt, O. S. *et al.* Mortality in sickle cell disease. Life expectancy and risk factors for early death. *N Engl J Med* **330**, 1639-1644. (1994).

3 Origa, R. beta-Thalassemia. *Genetics in medicine : official journal of the American College of Medical Genetics* **19**, 609-619, doi:10.1038/gim.2016.173 (2017).

4 Dedoussis, G. V., Sinopoulou, K., Gyparaki, M. & Loutradis, A. Fetal hemoglobin expression in the compound heterozygous state for -117 (G-->A) Agamma HPFH and IVSII-745 (C-->G) beta+ thalassemia: a case study. *Am J Hematol* **61**, 139-143, doi:10.1002/(SICI)1096-8652(199906)61:2<139::AID-AJH12>3.0.CO;2-7 [pii] (1999).

5 Dedoussis, G. V., Sinopoulou, K., Gyparaki, M. & Loutradis, A. Fetal hemoglobin expression in the compound heterozygous state for -117 (G-->A) Agamma HPFH and IVS-1 nt 110 (G-->A) beta+ thalassemia: a case study. *Eur J Haematol* **65**, 93-96 (2000).

6 Marcus, S. J., Kinney, T. R., Schultz, W. H., O'Branski, E. E. & Ware, R. E. Quantitative analysis of erythrocytes containing fetal hemoglobin (F cells) in children with sickle cell disease. *Am J Hematol* **54**, 40-46, doi:10.1002/(SICI)1096-8652(199701)54:1<40::AID-AJH6>3.0.CO;2-4 [pii] (1997).

7 Olivieri, N. F. & Weatherall, D. J. The therapeutic reactivation of fetal haemoglobin. *Hum Mol Genet* **7**, 1655-1658, doi:ddb180 [pii] (1998).

8 Papadakis, M. N., Patrinos, G. P., Tsaftaridis, P. & Loutradi-Anagnostou, A. A comparative study of Greek nondeletional hereditary persistence of fetal hemoglobin and beta-thalassemia compound heterozygotes. *J Mol Med* **80**, 243-247, doi:10.1007/s00109-001-0312-4 (2002).

9 Yu, L., Myers, G. & Engel, J. D. Small molecule therapeutics to treat the beta-globinopathies. *Curr Opin Hematol* **27**, 129-140, doi:10.1097/MOH.0000000000000579 (2020).

10 Fritsch, E. F., Lawn, R. M. & Maniatis, T. Molecular cloning and characterization of the human b-like globin gene cluster. *Cell* **19**, 959-972. (1980).

11 Grosveld, F., van Assendelft, G. B., Greaves, D. R. & Kollias, G. Position-independent, high-level expression of the human beta-globin gene in transgenic mice. *Cell* **51**, 975-985 (1987).

12 Forrester, W. C., Takegawa, S., Papayannopoulou, T., Stamatoyannopoulos, G. & Groudine, M. Evidence for a locus activation region: the formation of developmentally stable hypersensitive sites in globin-expressing hybrids. *Nucleic acids research* **15**, 10159-10177 (1987).

13 Stamatoyannopoulos, G. Control of globin gene expression during development and erythroid differentiation. *Exp Hematol* **33**, 259-271, doi:10.1016/j.exphem.2004.11.007 (2005).

14 Choi, O. R. & Engel, J. D. Developmental regulation of beta-globin gene switching. *Cell* **55**, 17-26 (1988).

15 Peterson, K. R. *et al.* Effect of deletion of 5'HS3 or 5'HS2 of the human beta-globin locus control region on the developmental regulation of globin gene expression in beta-globin locus yeast artificial chromosome transgenic mice. *Proc. Natl. Acad. Sci. U.s.a.* **93**, 6605-6609 (1996).

16 Bungert, J. *et al.* Synergistic regulation of human beta-globin gene switching by locus control region elements HS3 and HS4. *Genes & development* **9**, 3083-3096 (1995).

17 Tanimoto, K., Liu, Q., Bungert, J. & Engel, J. D. Effects of altered gene order or orientation of the locus control region on human beta-globin gene expression in mice. *Nature* **398**, 344-348 (1999).

18 Wijgerde, M., Grosveld, F. & Fraser, P. Transcription complex stability and chromatin dynamics in vivo. *Nature* **377**, 209-213 (1995).

19 Dillon, N. & Grosveld, F. Human gamma-globin genes silenced independently of other genes in the beta-globin locus. *Nature* **350**, 252-254 (1991).

20 Raich, N. *et al.* Autonomous developmental control of human embryonic globin gene switching in transgenic mice. *Science* **250**, 1147-1149 (1990).

21 Tanabe, O. *et al.* An embryonic/fetal beta-type globin gene repressor contains a nuclear receptor TR2/TR4 heterodimer. *EMBO J* **21**, 3434-3442, doi:10.1093/emboj/cdf340 (2002).

22 Tanabe, O. *et al.* Embryonic and fetal beta-globin gene repression by the orphan nuclear receptors, TR2 and TR4. *EMBO J* **26**, 2295-2306, doi:7601676 [pii] 10.1038/sj.emboj.7601676 (2007).

23 Martyn, G. E. *et al.* Natural regulatory mutations elevate the fetal globin gene via disruption of BCL11A or ZBTB7A binding. *Nat Genet* **50**, 498-503, doi:10.1038/s41588-018-0085-0 (2018).

24 Chen, Z. *et al.* A T-to-G transversion at nucleotide -567 upstream of HBG2 in a GATA-1 binding motif is associated with elevated hemoglobin F. *Mol Cell Biol* **28**, 4386-4393, doi:MCB.00071-08 [pii]10.1128/MCB.00071-08 (2008).

25 Xu, J. *et al.* Corepressor-dependent silencing of fetal hemoglobin expression by BCL11A. *Proc Natl Acad Sci U S A* **110**, 6518-6523, doi:10.1073/pnas.1303976110 (2013).

26 Yu, L. *et al.* BAP1 regulation of the key adaptor protein NCoR1 is critical for gamma-globin gene repression. *Genes & development* **32**, 1537-1549, doi:10.1101/gad.318436.118 (2018).

27 Shi, L., Cui, S., Engel, J. D. & Tanabe, O. Lysine-specific demethylase 1 is a therapeutic target for fetal hemoglobin induction. *Nature medicine* **19**, 291-294, doi:10.1038/nm.3101 (2013).

28 Hosseini, A. & Minucci, S. A comprehensive review of lysine-specific demethylase 1 and its roles in cancer. *Epigenomics* **9**, 1123-1142, doi:10.2217/epi-2017-0022 (2017).

29 Magliulo, D., Bernardi, R. & Messina, S. Lysine-Specific Demethylase 1A as a Promising Target in Acute Myeloid Leukemia. *Front Oncol* **8**, 255, doi:10.3389/fonc.2018.00255 (2018).

30 Ibanez, V. *et al.* Efficacy and safety of long-term RN-1 treatment to increase HbF in baboons. *Blood* **129**, 260-263, doi:10.1182/blood-2016-10-746727 (2017).

31 Rivers, A. *et al.* The LSD1 inhibitor RN-1 recapitulates the fetal pattern of hemoglobin synthesis in baboons (P. anubis). *Haematologica* **101**, 688-697, doi:10.3324/haematol.2015.140749 (2016).

32 Cui, S. *et al.* The LSD1 inhibitor RN-1 induces fetal hemoglobin synthesis and reduces disease pathology in sickle cell mice. *Blood* **126**, 386-396, doi:10.1182/blood-2015-02-626259 (2015).

33 Kerenyi, M. A. *et al.* Histone demethylase Lsd1 represses hematopoietic stem and progenitor cell signatures during blood cell maturation. *eLife* **2**, e00633, doi:10.7554/eLife.00633 (2013).

34 Sprussel, A. *et al.* Lysine-specific demethylase 1 restricts hematopoietic progenitor proliferation and is essential for terminal differentiation. *Leukemia*, doi:10.1038/leu.2012.157 leu2012157 [pii] (2012).

35 Giarratana, M. C. *et al.* Ex vivo generation of fully mature human red blood cells from hematopoietic stem cells. *Nat Biotechnol* **23**, 69-74 (2005).

36 Giarratana, M. C. *et al.* Proof of principle for transfusion of in vitro-generated red blood cells. *Blood* **118**, 5071-5079, doi:10.1182/blood-2011-06-362038 (2011).

37 Li, J. *et al.* Isolation and transcriptome analyses of human erythroid progenitors: BFU-E and CFU-E. *Blood* **124**, 3636-3645, doi:10.1182/blood-2014-07-588806 (2014).

38 Kuhn, R., Schwenk, F., Aguet, M. & Rajewsky, K. Inducible gene targeting in mice. *Science* **269**, 1427-1429 (1995).

39 Heinrich, A. C., Pelanda, R. & Klingmuller, U. A mouse model for visualization and conditional mutations in the erythroid lineage. *Blood* **104**, 659-666 (2004).

40 Georgiades, P. *et al.* VavCre transgenic mice: a tool for mutagenesis in hematopoietic and endothelial lineages. *Genesis* **34**, 251-256, doi:10.1002/gene.10161 (2002).

41 Yu, L. *et al.* Derepression of the DNA Methylation Machinery of the Gata1 Gene Triggers the Differentiation Cue for Erythropoiesis. *Mol Cell Biol* **37**, doi:10.1128/MCB.00592-16 (2017).

42 Suzuki, M., Moriguchi, T., Ohneda, K. & Yamamoto, M. Differential contribution of the Gata1 gene hematopoietic enhancer to erythroid differentiation. *Mol Cell Biol* **29**, 1163-1175, doi:10.1128/MCB.01572-08 (2009).

43 Takai, J. *et al.* The Gata1 5' region harbors distinct cis-regulatory modules that direct gene activation in erythroid cells and gene inactivation in HSCs. *Blood* **122**, 3450-3460, doi:10.1182/blood-2013-01-476911 (2013).

44 Lim, K. C. *et al.* Conditional Gata2 inactivation results in HSC loss and lymphatic mispatterning. *The Journal of clinical investigation* **122**, 3705-3717, doi:10.1172/JCI61619 (2012).

45 Madisen, L. *et al.* A robust and high-throughput Cre reporting and characterization system for the whole mouse brain. *Nat Neurosci* **13**, 133-140, doi:10.1038/nn.2467 (2010).

46 Chen, K. *et al.* Resolving the distinct stages in erythroid differentiation based on dynamic changes in membrane protein expression during erythropoiesis. *Proc Natl Acad Sci U S A* **106**, 17413-17418, doi:0909296106 [pii] 10.1073/pnas.0909296106 (2009).

47 Shimizu, R., Engel, J. D. & Yamamoto, M. GATA1-related leukaemias. *Nat Rev Cancer* **8**, 279-287, doi:10.1038/nrc2348 (2008).

48 Pronk, C. J. *et al.* Elucidation of the phenotypic, functional, and molecular topography of a myeloerythroid progenitor cell hierarchy. *Cell Stem Cell* **1**, 428-442, doi:10.1016/j.stem.2007.07.005 (2007).

49 Arinobu, Y. *et al.* Reciprocal activation of GATA-1 and PU.1 marks initial specification of hematopoietic stem cells into myeloerythroid and myelolymphoid lineages. *Cell Stem Cell* **1**, 416-427, doi:10.1016/j.stem.2007.07.004 (2007).

50 Wang, J. *et al.* Opposing LSD1 complexes function in developmental gene activation and repression programmes. *Nature* **446**, 882-887, doi:nature05671 [pii] 10.1038/nature05671 (2007).

51 Riccardi, C. & Nicoletti, I. Analysis of apoptosis by propidium iodide staining and flow cytometry. *Nat Protoc* **1**, 1458-1461, doi:10.1038/nprot.2006.238 (2006).

52 Laslo, P. *et al.* Multilineage transcriptional priming and determination of alternate hematopoietic cell fates. *Cell* **126**, 755-766, doi:10.1016/j.cell.2006.06.052 (2006).

53 Scott, E. W., Simon, M. C., Anastasi, J. & Singh, H. Requirement of transcription factor PU.1 in the development of multiple hematopoietic lineages. *Science* **265**, 1573-1577 (1994).

54 Rosenbauer, F. & Tenen, D. G. Transcription factors in myeloid development: balancing differentiation with transformation. *Nat Rev Immunol* **7**, 105-117, doi:10.1038/nri2024 (2007).

55 Willcockson, M. A. *et al.* Runx1 promotes murine erythroid progenitor proliferation and inhibits differentiation by preventing Pu.1 downregulation. *Proc Natl Acad Sci U S A* **116**, 17841-17847, doi:10.1073/pnas.1901122116 (2019).

56 Kurita, R. *et al.* Establishment of immortalized human erythroid progenitor cell lines able to produce enucleated red blood cells. *PLoS One* **8**, e59890, doi:10.1371/journal.pone.0059890 (2013).

57 Cunningham, L. *et al.* Identification of benzodiazepine Ro5-3335 as an inhibitor of CBF leukemia through quantitative high throughput screen against RUNX1-CBFbeta interaction. *Proc Natl Acad Sci U S A* **109**, 14592-14597, doi:10.1073/pnas.1200037109 (2012).

58 Illendula, A. *et al.* Small Molecule Inhibitor of CBFbeta-RUNX Binding for RUNX Transcription Factor Driven Cancers. *EBioMedicine* **8**, 117-131, doi:10.1016/j.ebiom.2016.04.032 (2016).

59 Chou, S. T. *et al.* Graded repression of PU.1/Sfpi1 gene transcription by GATA factors regulates hematopoietic cell fate. *Blood* **114**, 983-994, doi:10.1182/blood-2009-03-207944 (2009).

60 Guo, Y. *et al.* GATA2 regulates GATA1 expression through LSD1-mediated histone modification. *Am J Transl Res* **8**, 2265-2274 (2016).

61 Moreau-Gachelin, F., Tavitian, A. & Tambourin, P. Spi-1 is a putative oncogene in virally induced murine erythroleukaemias. *Nature* **331**, 277-280, doi:10.1038/331277a0 (1988).

62 Fang, Y., Liao, G. & Yu, B. LSD1/KDM1A inhibitors in clinical trials: advances and prospects. *J Hematol Oncol* **12**, 129, doi:10.1186/s13045-019-0811-9 (2019).

63 Wass, M. *et al.* A proof of concept phase I/II pilot trial of LSD1 inhibition by tranylcypromine combined with ATRA in refractory/relapsed AML patients not eligible for intensive therapy. *Leukemia*, doi:10.1038/s41375-020-0892-z (2020).

64 Brandt, W. *et al.* Defining the functional boundaries of the Gata2 locus by rescue with a linked bacterial artificial chromosome transgene. *J Biol Chem* **283**, 8976-8983, doi:M709364200 [pii]10.1074/jbc.M709364200 (2008).

65 Yu, L. *et al.* GATA2 regulates body water homeostasis through maintaining aquaporin 2 expression in renal collecting ducts. *Mol Cell Biol* **34**, 1929-1941, doi:10.1128/MCB.01659-13 (2014).

66 Moriguchi, T. *et al.* The Human GATA1 Gene Retains a 5' Insulator That Maintains Chromosomal Architecture and GATA1 Expression Levels in Splenic Erythroblasts. *Mol Cell Biol* **35**, 1825-1837, doi:10.1128/MCB.00011-15 (2015).

Supplemental Information

Supplemental Figure 1: Characterization of Inhibitor Effects on Human CD34+ HSPC-induced Erythroid Differentiation. (A) LSD1 inhibition by a novel, reversible LSD1 inhibitor, CCG50 (LSDi). (B) Schematic summarizing the timing and duration of additives (hydrocortisone, IL3, SCF and EPO) media supplements during *in vitro* erythroid differentiation of human CD34+ HSPCs. Hydrocortisone and human IL-3 were withdrawn on day7 when the LSD1 inhibitor(s) were added; human SCF was withdrawn from culture media on day11. (C) Representative flow cytometric cell count of CD34+ HSPCs undergoing erythroid differentiation at d7 (prior to LSD1 inhibitor treatment) analyzed with anti-CD71 and anti-CD235a erythroid antibodies.

Supplemental Figure 2: Mouse *Gata1* BAC recombination diagram. A creER^{T2}-PolyA-Neo cassette (Takai et al. 2013; Yu et al. 2017) was targeted to the ATG start codon in exon 2 of a 196 kb wild type mouse *Gata1* BAC (*G1B*). Subsequently, the Neo selection cassette was removed from the recombinant *G1B*CreER^{T2}-Neo BAC to generate the resultant *G1B*CreER^{T2} BAC, which was used to generate two lines of transgenic mice.

Supplemental Figure 3: *G1B*CreERT2 is not active in bone marrow non-erythroid lineages. TdTomato epifluorescence was not detectable in B220+, Gr1+, CD11b+ or CD3e+ cells in the BM of *G1B*CreER^{T2} lines L245 and L259 treated with Tamoxifen (red peak). R26T:*G1B*CreER^{T2} mice that were not treated with Tx served as negative controls (blue peak).

Supplemental Figure 4: *G1B*CreER^{T2} is expressed in a minor fraction of megakaryocytes and mast cells. Representative flow cytometric plots depicting the gating cutoffs for megakaryocytic progenitor cells (MkPs; Lin-cKit+Sca1-CD41+CD150+; A, B), megakaryocytes (Mk; CD61+CD41+; C, D) and mast cells (FceRIa+c-Kit+; E, F) in the BM of

untreated (left panels in A, C and E; blue peaks in B, D and F) or Tx-treated (right panels in A, C and E; red peaks in B, D and F) R26T:*G1B*CreER^{T2} L259 mice. Representative flow histograms depict TdTomato signal (red peaks) in very few MkPs (B), Mk (D) or mast cells (F).

Supplemental Figure 5: Gating strategies for CFU-E and megakaryocytic progenitor cell populations. Total BM cells from untreated (left panels) or Tx-treated (right panels) R26T:*G1B*CreER^{T2} L259 mice were stained with the indicated lineage antibodies. Representative flow plots showing gating cutoffs for CFU-Es (Lin-cKit+Sca1-CD41-CD16/32-CD150-CD105+) and megakaryocytic progenitors **(**MkPs; Lin-cKit+Sca1-CD41+CD150+), which were analyzed for TdTomato epifluorescence in Fig.s 2C and S4, respectively.

Supplemental Figure 6: Gating strategies for LSK, CMP, GMP and MEP cell populations. Total BM cells from untreated (left panels) or Tx-treated (right panels) R26T:*G1B*CreER^{T2} L259 mice were stained with Lineage-, c-Kit-, Sca1-, CD34- or CD16/32 antibodies. Representative flow plots showing gating strategies defining the LSK **(**Lin-c-Kit+Sca1+), CMP **(**Lin-c-Kit+Sca1-CD16/32-CD34+), GMP (Lin-c-Kit+Sca1-CD16/32+CD34+) and MEP (Lin-c-Kit+Sca1-CD16/32-CD34-) populations, which were further analyzed for TdTomato epifluorescence in Fig. 2C.

Supplemental Figure 7: Gating strategies for CMP, GMP and MEP populations. The CD41-CD16/32- LK fraction was separated by CD105 and CD150 for CFU-E staining as shown in Figure 3. The LK fraction was separated by CD34 and CD16/32 for CMP, GMP and MEP staining in Figure 4.

Supplemental Figure 8: CFU-E cell death is comparable in *Lsd1*-CKO and control mice. The cell death of CFU-E cells in Figure 3D was analyzed by AnnexinV staining.

Supplemental Figure 9: Erythroid precursor cells in *Lsd1*-CKO mice have diminished cell death. The apoptotic cell death of BasoE, PolyE and OrthoE in Figure 3F was analyzed by AnnexinV staining. Data is shown as the means ± SD. (** $p<0.01$; unpaired Student's t-test).

Supplemental Figure10: The cell cycle status of erythroid precursors in *Lsd1*-CKO and control mice is comparable. The distribution of CD71+Ter119+ cells depicted in Figure3F was analyzed by DAPI staining. Data is shown as the means ± SD. (** $p<0.01$; unpaired Student's t-test). 2N, cells in G1 phase of cell cycle; S, cells in S phase of cell cycle; 4N, cells in G2/M phase of the cell cycle.

Supplemental Figure11: GMP in *Lsd1*-CKO mice have significantly diminished cell death. The cell death of GMP shown in Figure 4A was analyzed by AnnexinV staining. Data was shown as the means ± SD. (** $p<0.01$; unpaired Student's t-test).

Supplemental Figure12: Sanger sequencing data of *Pu.1* -/- HUDEP2 clones. Individual HUDEP2 clones were subjected to genomic DNA extraction, the genomic DNA locus of sgRNA cutting sites were amplified by PCR, the amplicons were subcloned into sequencing vector and the sanger chromatogram data surrounding the cutting sites were shown. Note, clone P2-25 has two PCR products with different size; clone P3-14 and P3-18 have only one PCR product; and clone P2-4 has no PCR product, all PCR amplicons were sequenced.

Supplemental Figure13: Sanger sequencing data of Runx1 -/- clones. Each individual clones were subjected to genomic DNA extraction, the genomic DNA locus of sgRNA cutting sites were amplified by PCR, the amplicons were subcloned into sequencing vector and the sanger chromatogram data surrounding the cutting sites were shown.

Supplemental Figure 14. *Pu.1* or *Runx1* knockout rescues HUDEP2 cells from the side effects of LSD1 inhibition. CD71/CD235a flow cytometry analysis of three different non-specific sgRNA-infected cells (left), four *Pu.1*-/- clones (middle) or four *Runx1*-/- clones (right) treated with **(A)** DMSO or **(B)** 300 nM CCG50 LSD1i for four days after induction of erythroid differentiation.

Supplemental Figure 15. RUNX1 inhibitor co-treatment partially rescues the toxicity of LSD1 inhibitor CCG50. (A) Human CD34+ HSPC were expanded for 7 days; at day7, cells were reseeded and treated with LSD1 inhibitor CCG50, RUNX1 inhibitors (Ro5 or A-10-104) or inhibitors of both factors. **(B)** CD71/CD235a staining of differentiating human CD34+ cells in erythroid differentiation at day 9, 2 days after adding CCG50, RUNX1 inhibitor Ro5-3335, RUNX1 inhibitor AI-10-104 (A104) or both LSD1 and RUNX1 inhibitors.

Supplemental Table 1. Sequences of all DNA oligonucleotides used in these studies,

Supplemental Table 2. List of all antibodies, antigens recognized, and the suppliers used in these studies,

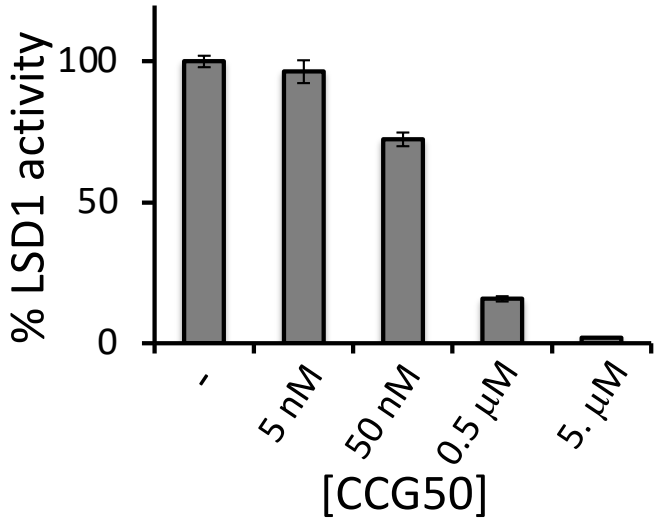

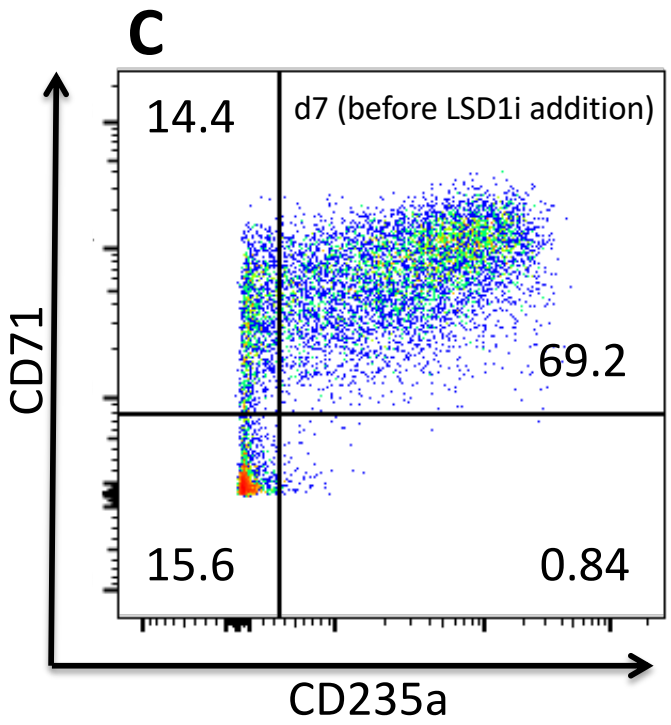

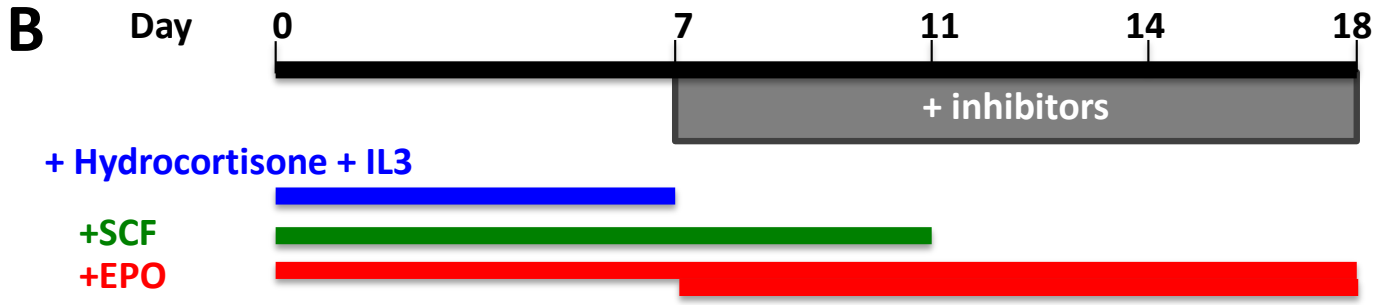

Flow Cytometry	D7	D11	D14	D18
RNA collection			D14	
HPLC Analysis				D18

Supplemental Figure 1.

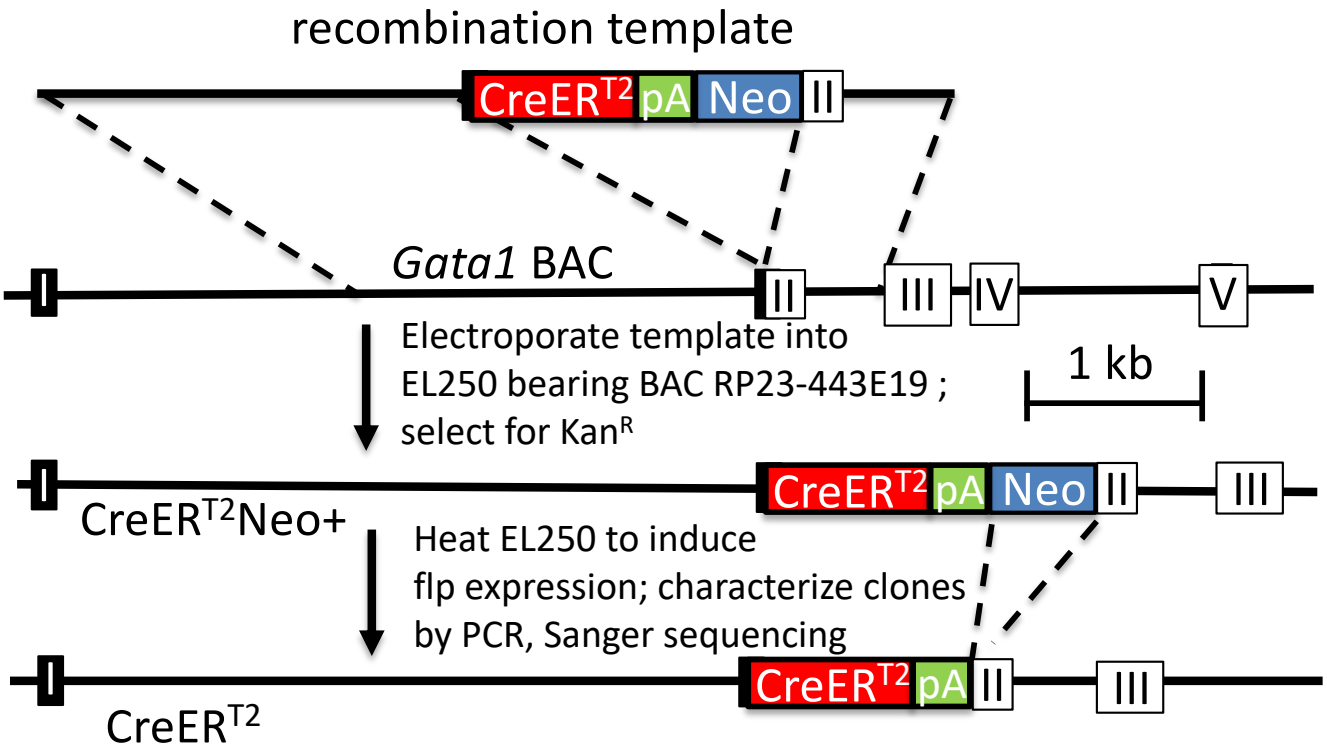

Supplemental Figure 2.

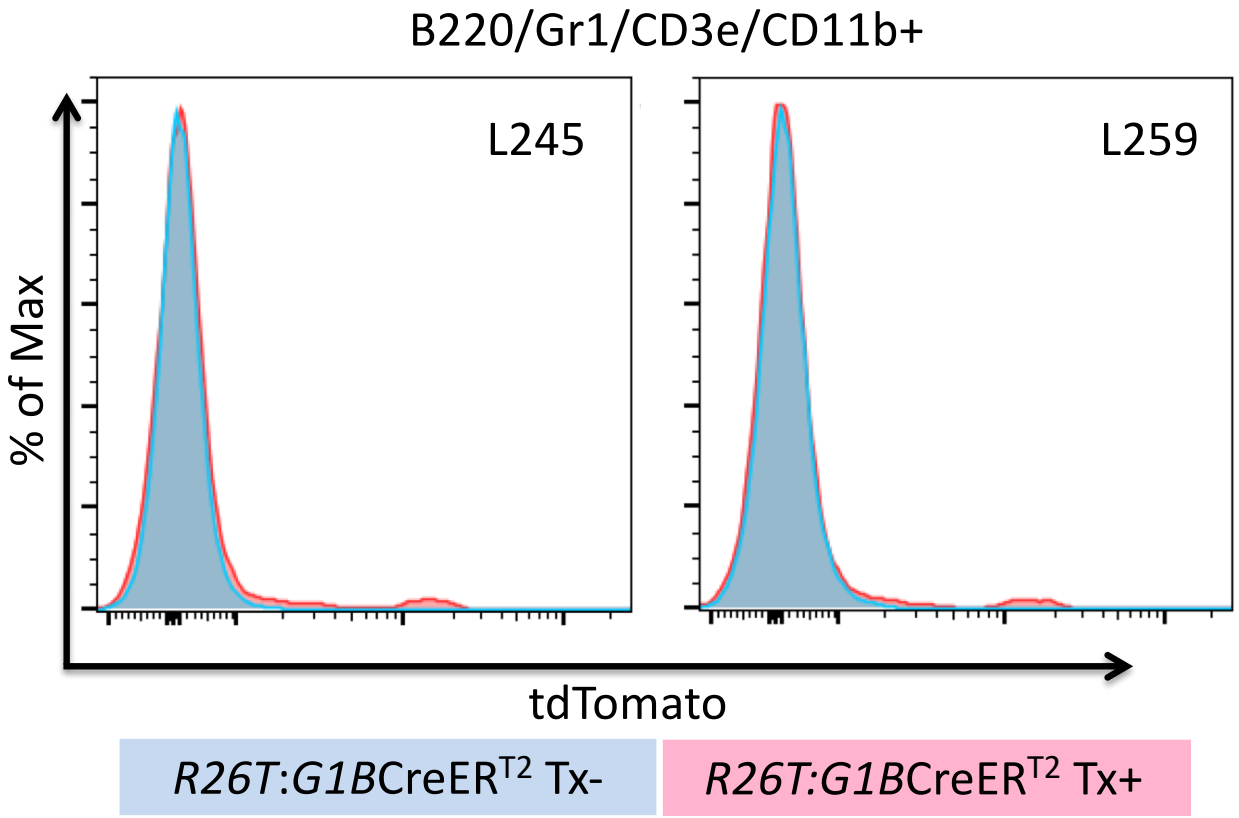

Supplemental Figure 3.

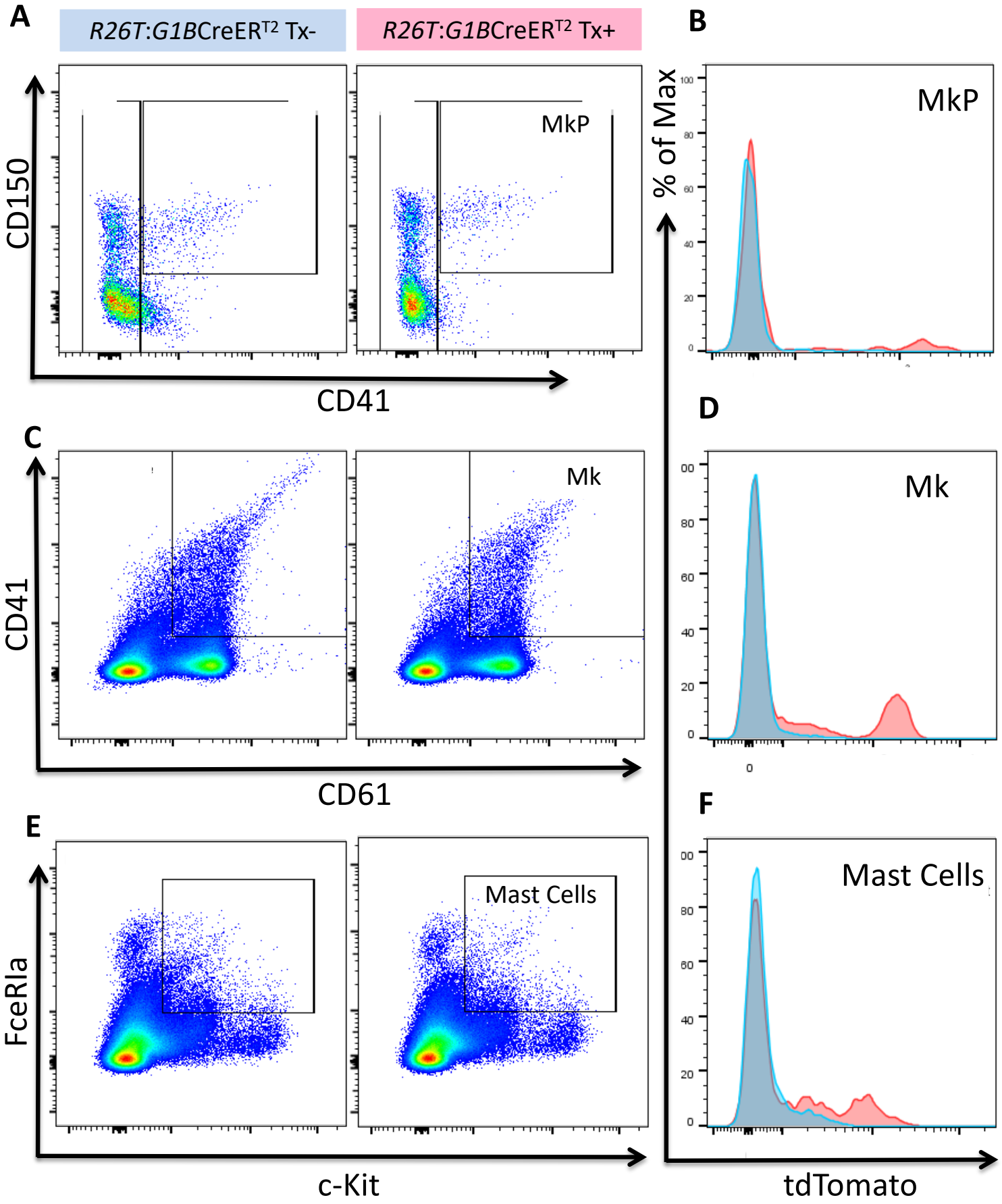

Supplemental Figure 4.

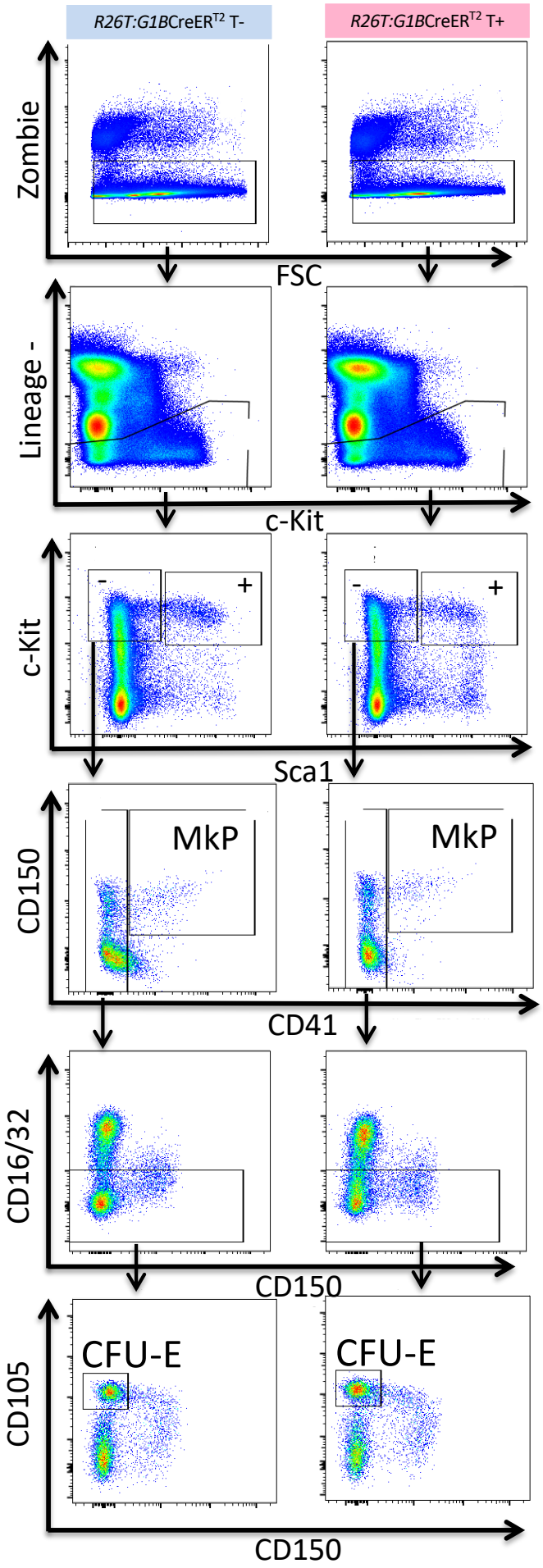

Supplemental Figure 5.

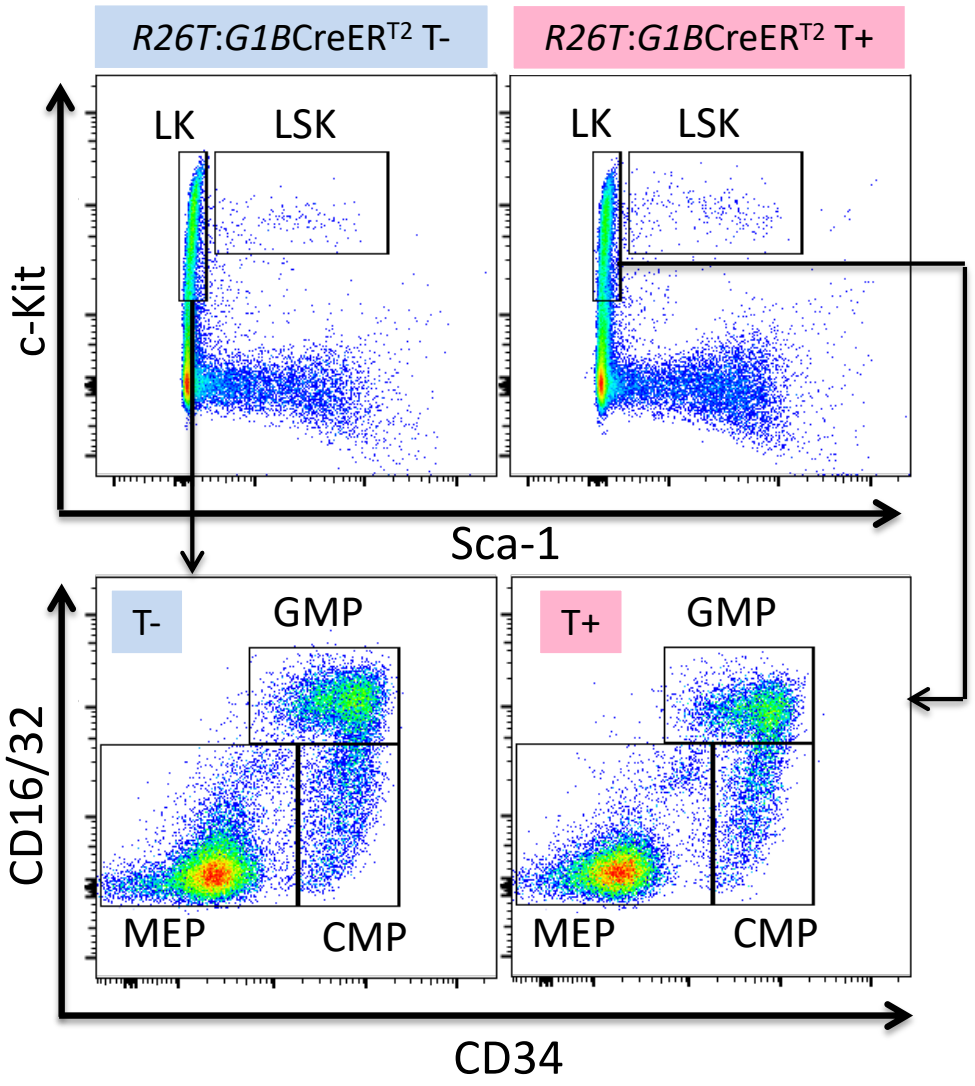

Supplemental Figure 6.

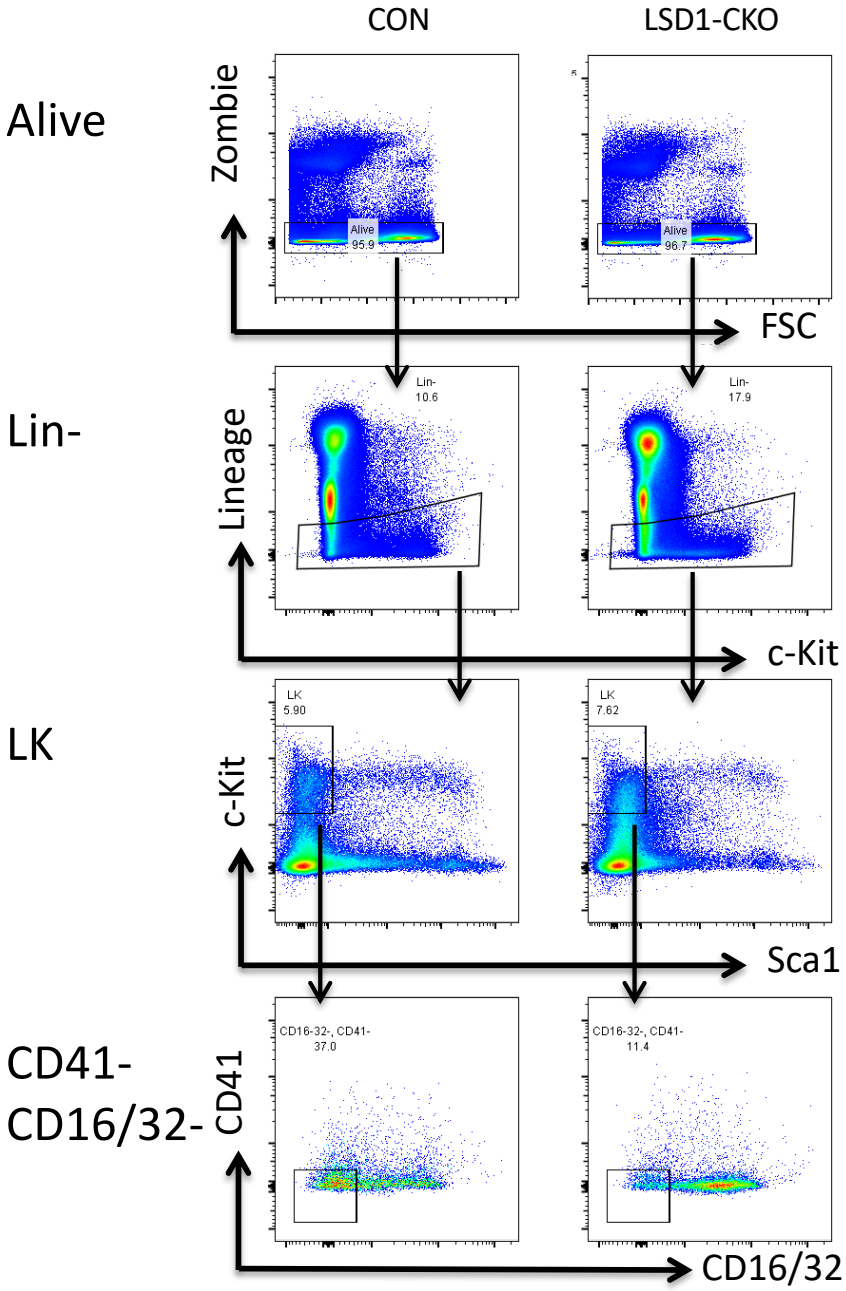

Supplemental Figure 7.

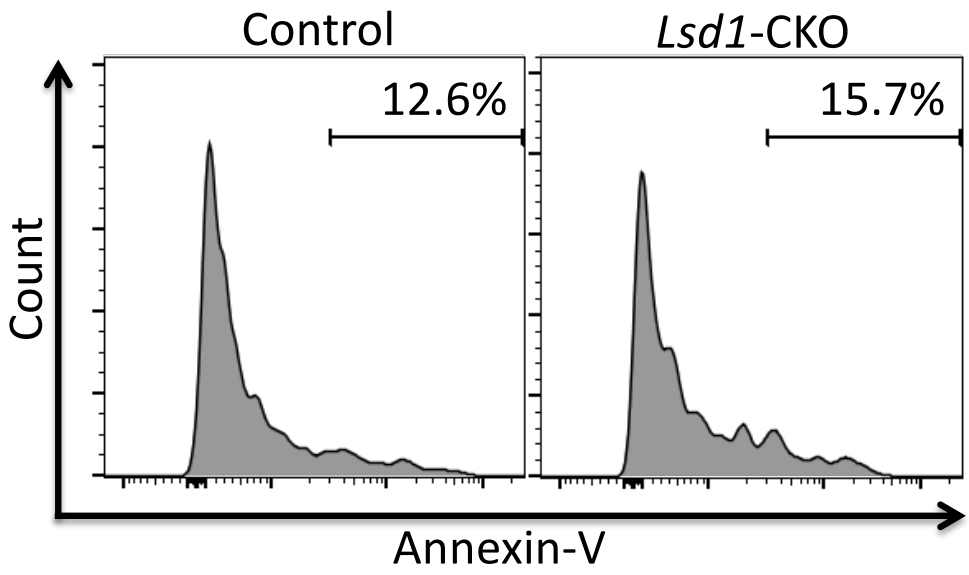

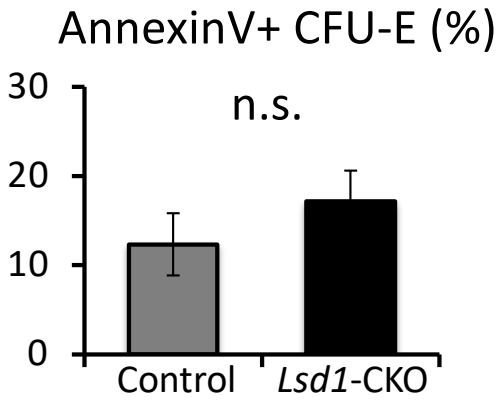

Supplemental Figure 8.

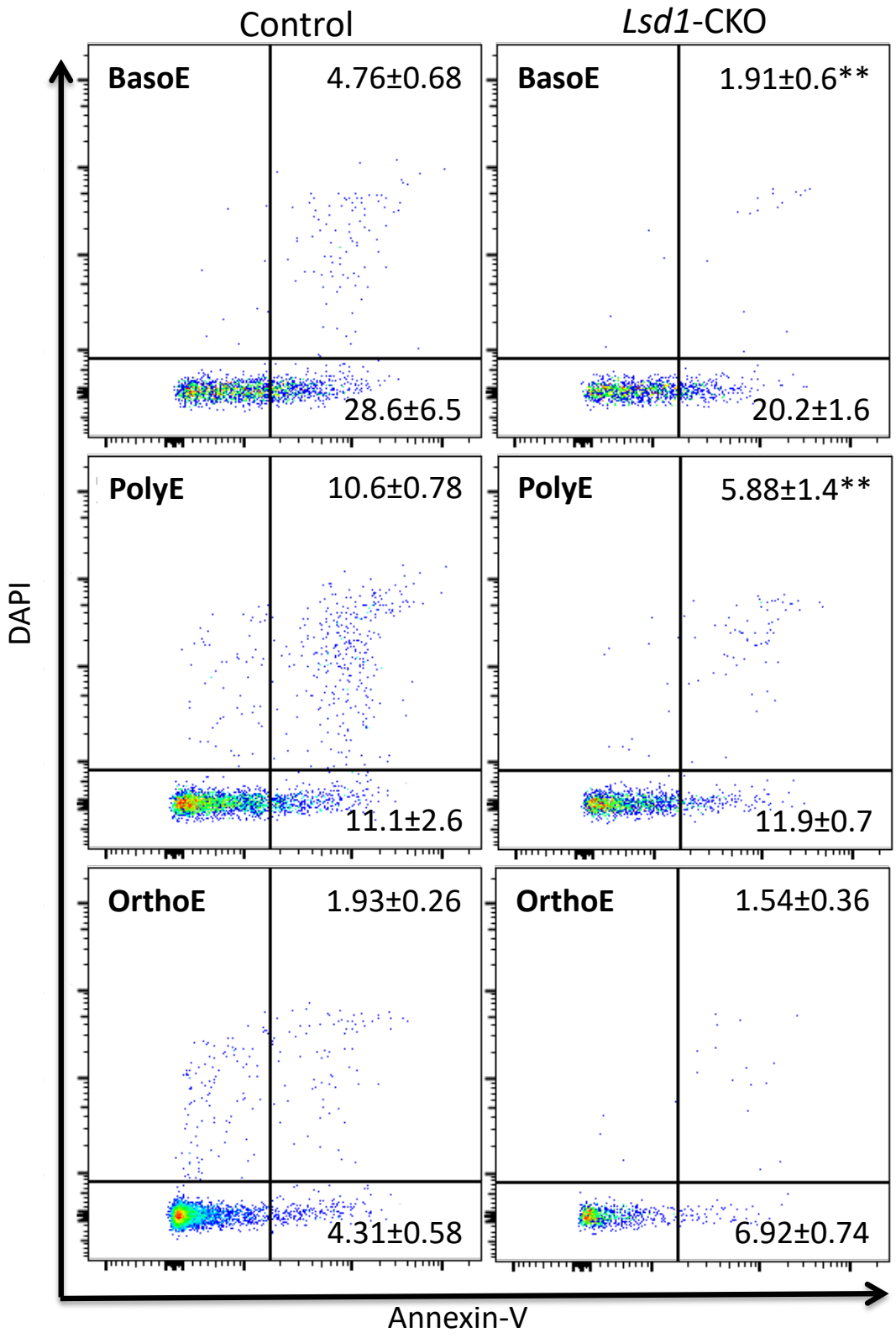

Supplemental Figure 9.

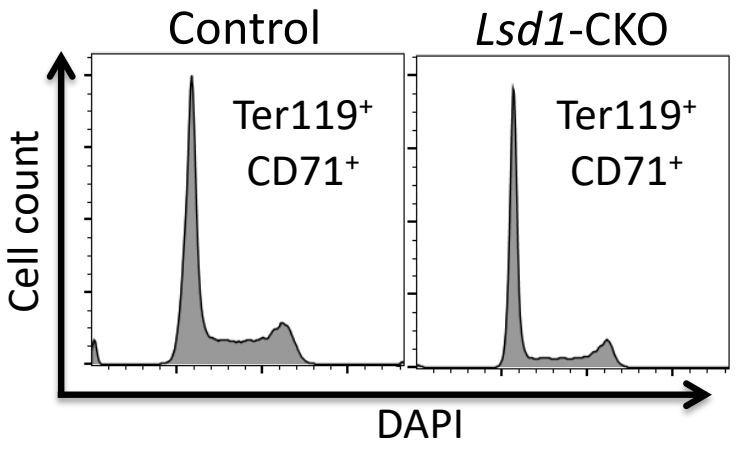

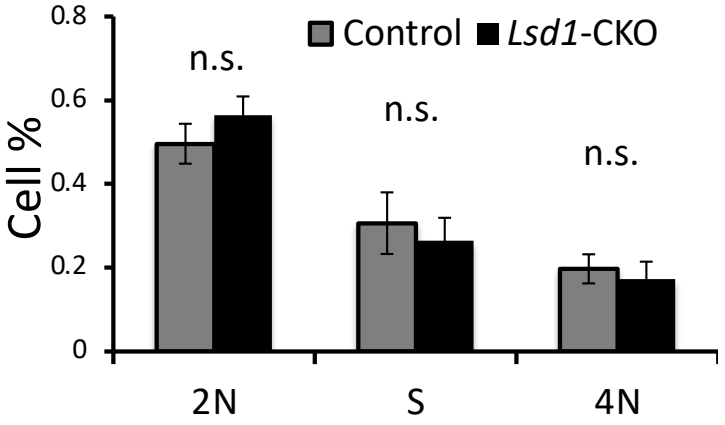

Supplemental Figure 10.

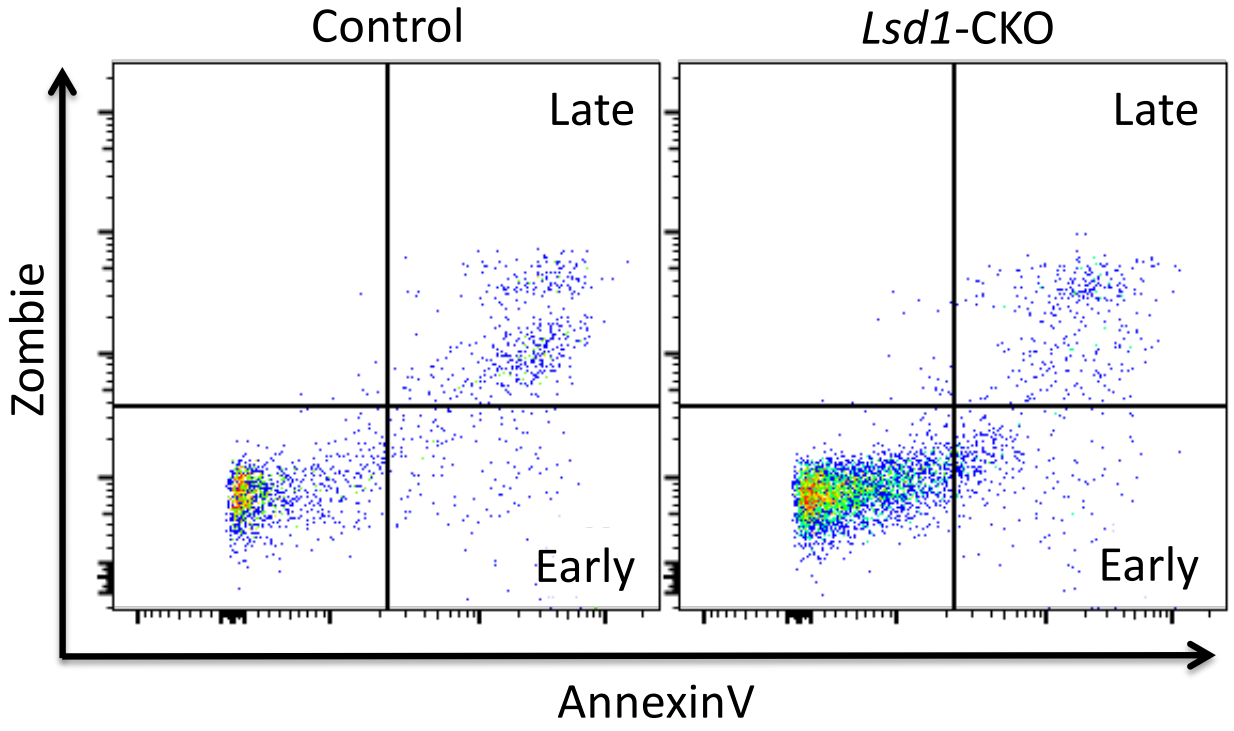

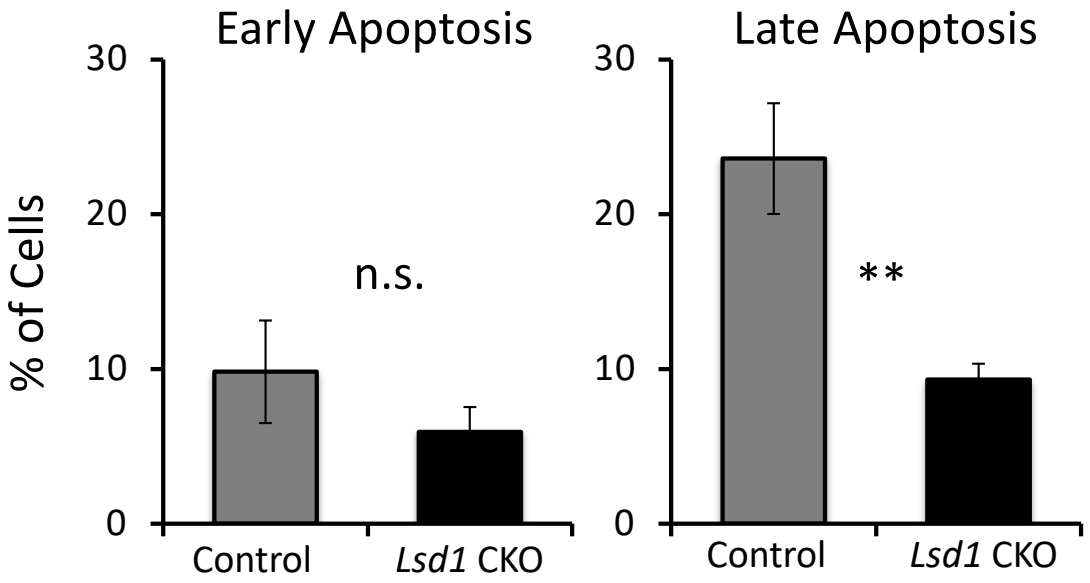

Supplemental Figure 11.

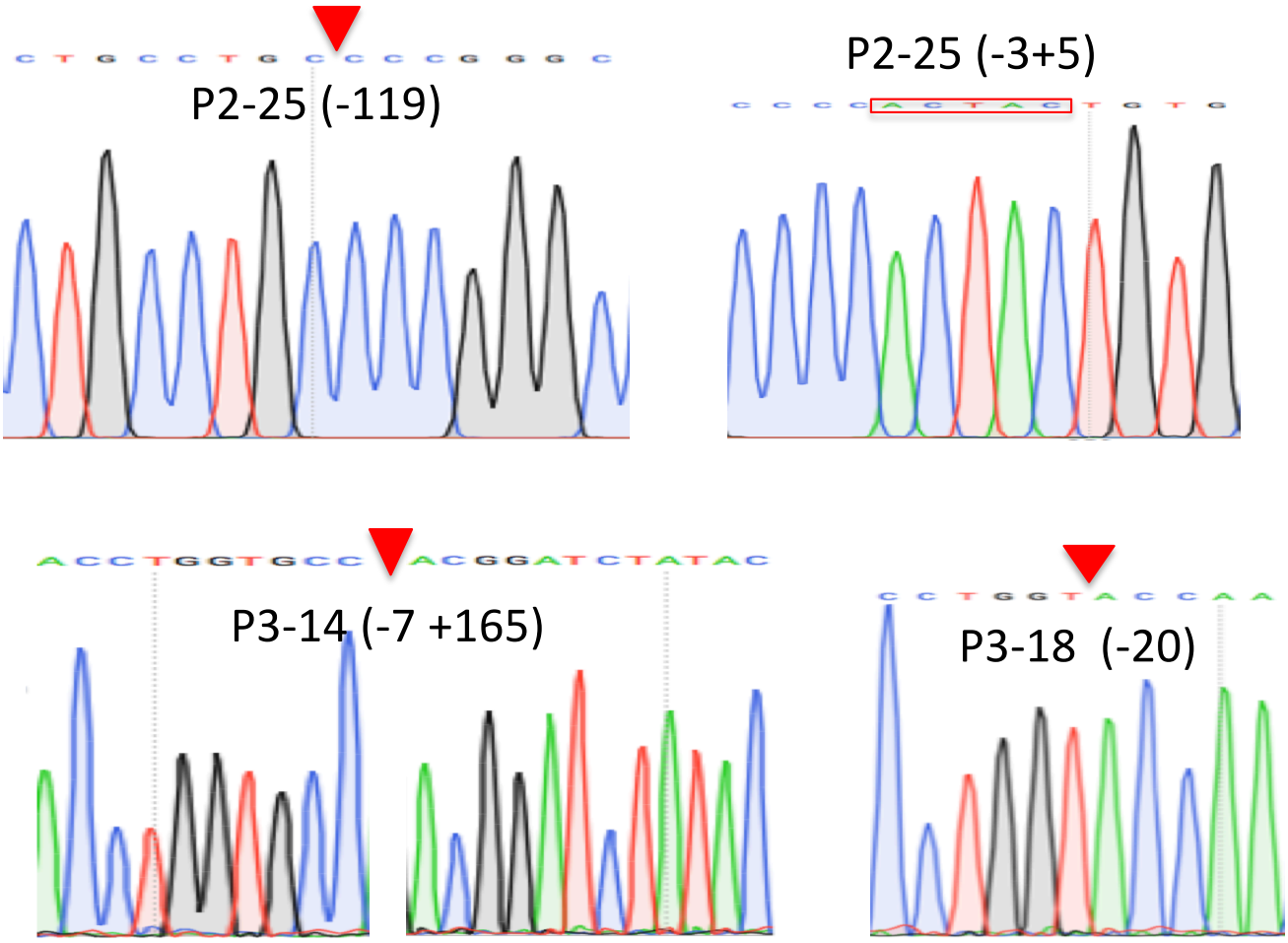

Supplemental Figure 12.

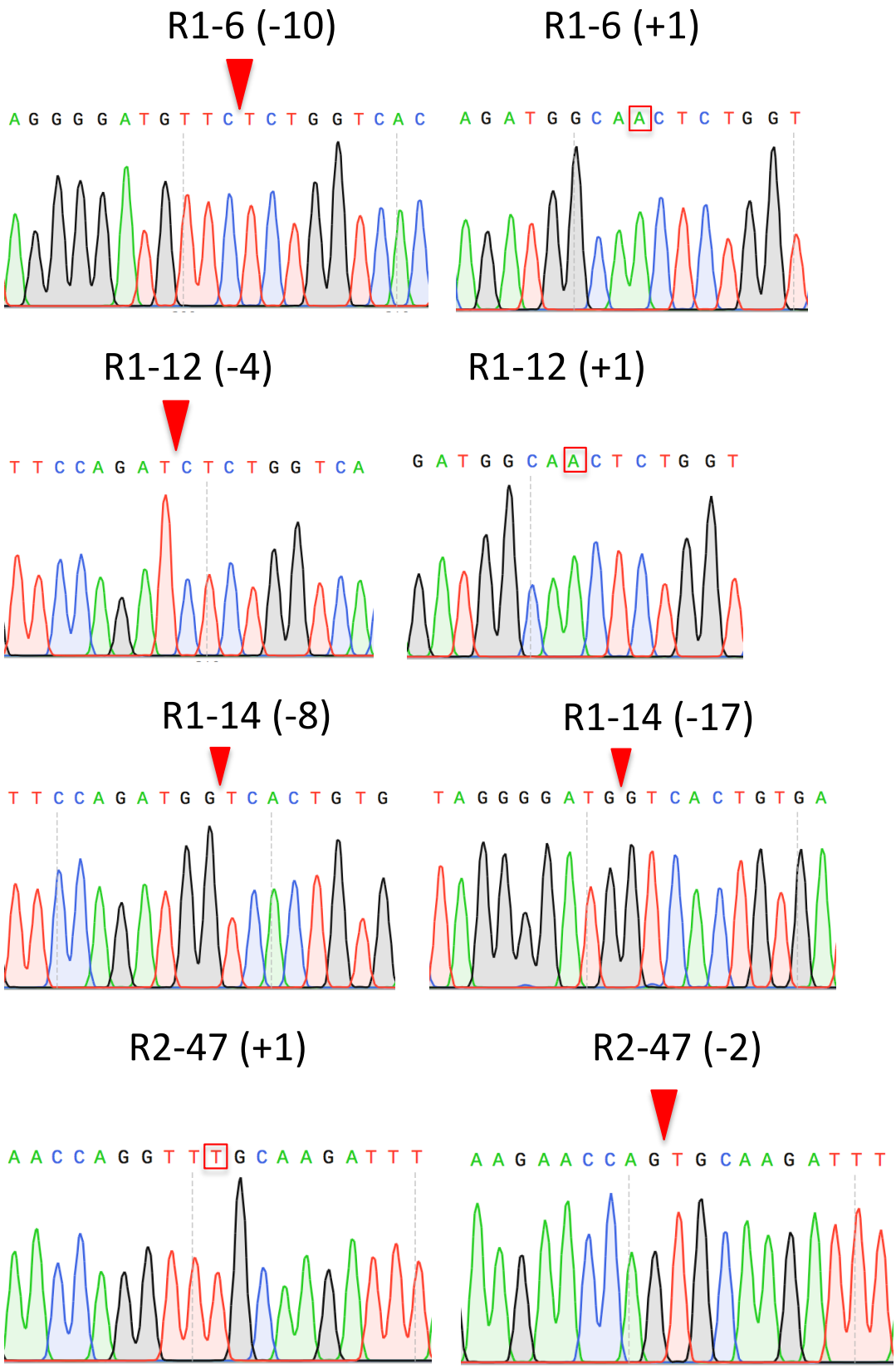

Supplemental Figure 13.

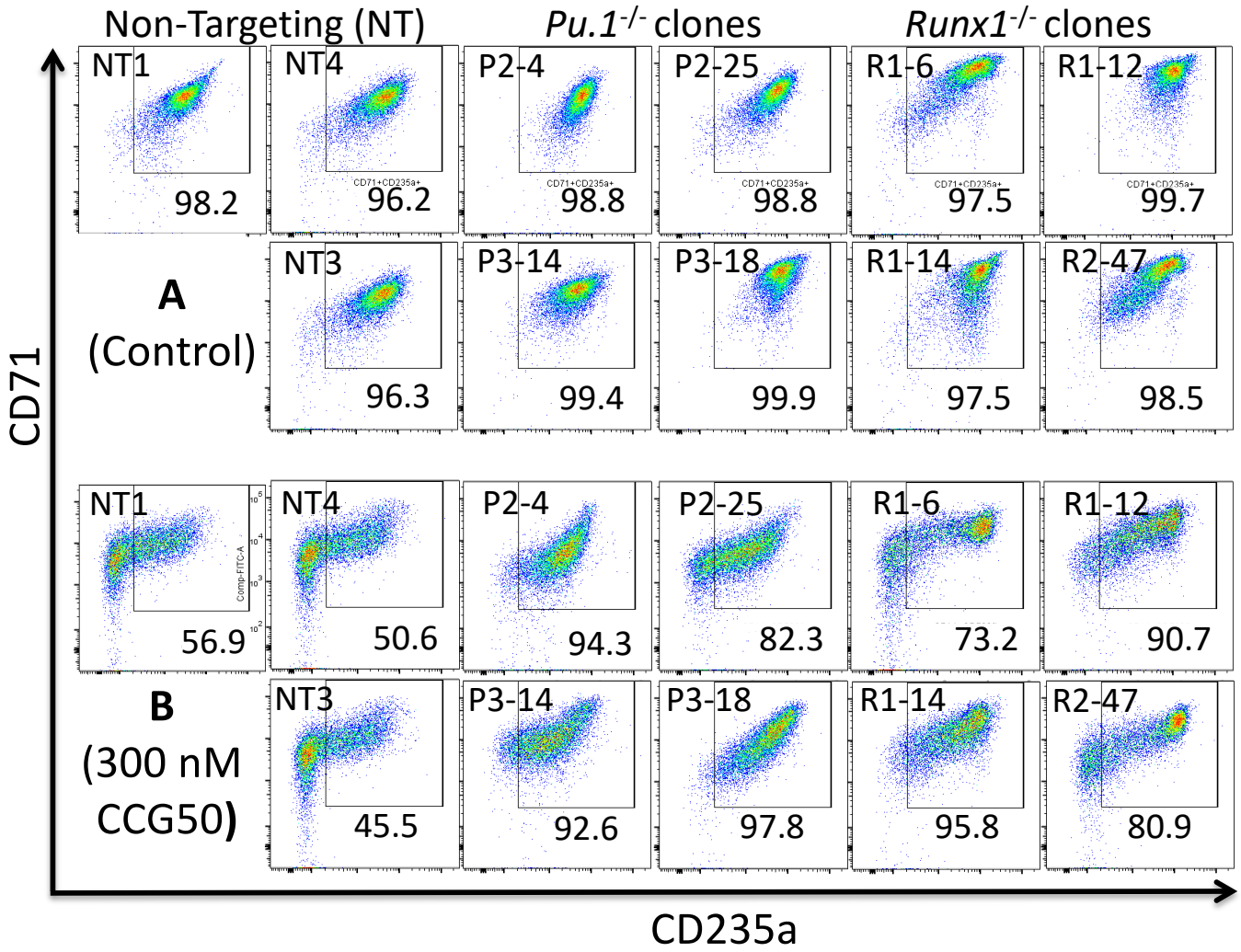

Supplemental Figure 14.

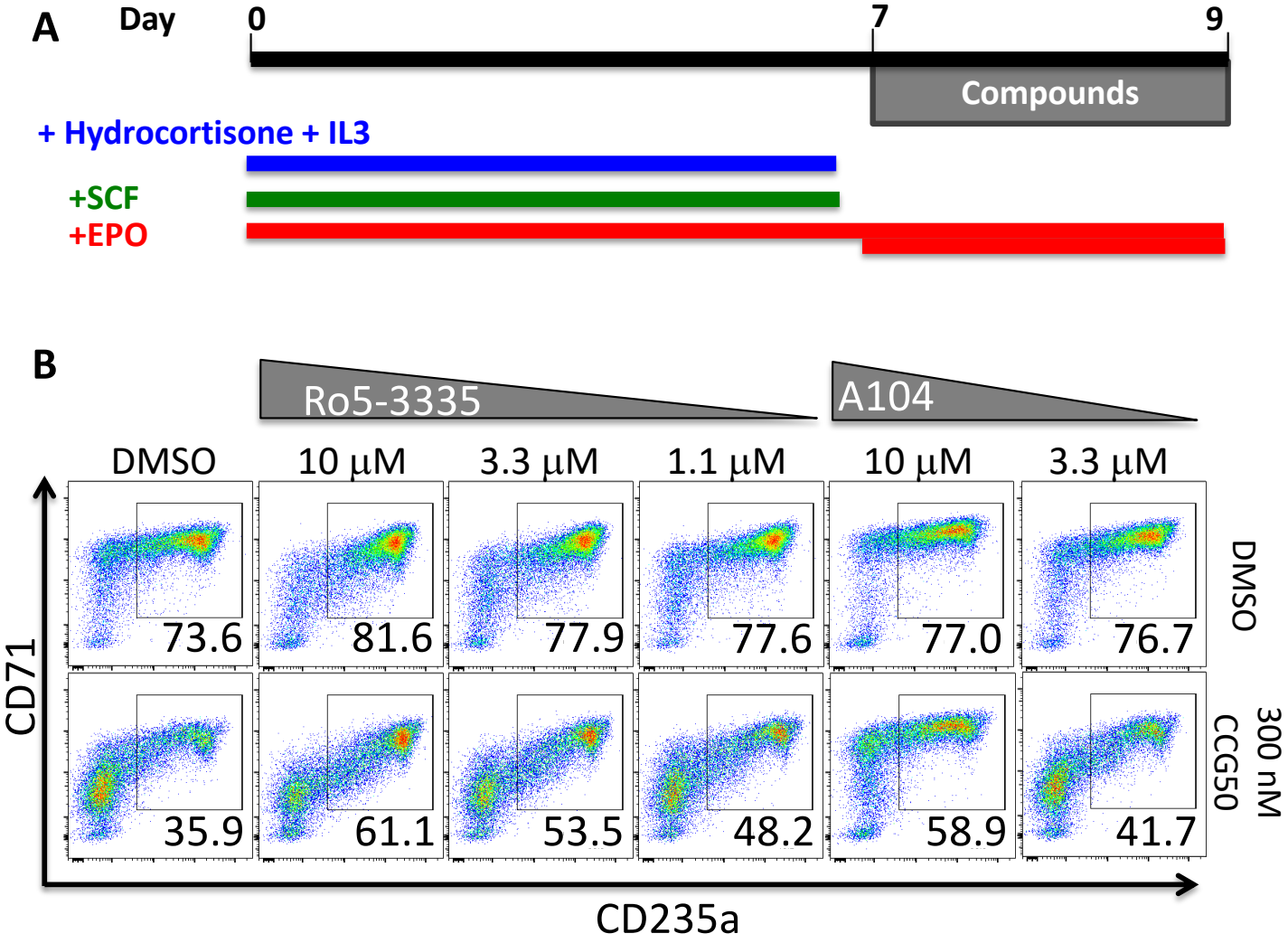

Supplemental Figure 15.

Supplemental Table 1: Oligonucleotide primers

Mouse Genotyping	**Forward 5' to 3'**	**Reverse 5' to 3'**
Lsd1 flox	AGCTACAGCACCAACACTAAAGAG	CAGCAGCTCGACAGCTACAGAGTT
CAT	CAGTCAGTTGCTCAATGTACC	ACTGGTGAAACTCACCCA
Cre	ACGTTCACCGGCATCAACGT	CTGCATTACCGGTCGATGCA
ERT2	GACAGGGAGCTGGTTCACAT	AGAGACTTCAGGGTGCTGGA
R26T	CTGTTCCTGTACGGCATGG	GGCATTAAAGCAGCGTATCC
Real time qPCR	**Forward 5' to 3'**	**Reverse 5' to 3'**
Human OAZ1	GACAGCTTTGCAGTTCTCCTGG	TTCGGAGCAAGGCGGCTC
Human γ-globin	TGGATCCTGAGAACTTCAAGC	CACTGGCCACTCCAGTCAC
Human β-globin	AGGAGAAGTCTGCCGTTACTG	CCGAGCACTTTCTTGCCATGA
Human GATA1	CACTGAGCTTGCCACATCC	ATGGAGCCTCTGGGGATTA
Human KLF1	GGGAGCCTCTTACGGAAAAT	TGCACGACAGTTTGGACATC
Human TAL1	GTACCCCCGTAGCGGAAA	AGGTGTCTACGCGGTTGC
Human PU.1	GACACGGATCTATACCAACGCC	CCGTGAAGTTGTTCTCGGCGAA
Human RUNX1	CCACCTACCACAGAGCCATCAA	TTCACTGAGCCGCTCGGAAAAG
Human CEBPA	GCAAATCGTGCCTTGTCAT	CTCATGGGGGTCTGCTGTAG
Mouse RUNX1	CACCGTCTTTACAAATCCGCCAC	CGCTCGGAAAAGGACAAACTCC
Mouse PU.1	GAGGTGTCTGATGGAGAAGCTG	ACCCACCAGATGCTGTCCTTCA
Mouse LSD1	CGATACTGTGCTTGTCCACCGA	CCAAGCCAGAAACACCTGAACC
Mouse GATA1	ACGACCACTACAACACTCTGGC	TTGCGGTTCCTCGTCTGGATTC
Mouse 18S rRNA	CTCAACACGGGAAACCTCAC	CGCTCCACCAACTAAGAACG
Lsd1 deletion P1	TCAGGTGTTTCTGGCTTGG	CTCTTACCCTGGCTTCCAGA
Lsd1 deletion P2	TAGTTAGGCAGGCAGCAGGT	GCAGCAGACATTGCTCAAAC
ChIP assay	**Forward 5' to 3'**	**Reverse 5' to 3'**
huPu.1 TSS	TCTCTTGCGCTACATACAGGAA	ATCCCTCTCAGTCCCAGCTT
huPu.1 Control	AAACCTCAGGGAAGGCTGAT	ACCAGGGATCTTACGCAGTC
***Gata1* BAC recombination**	**Forward 5' to 3'**	**Reverse 5' to 3'**
5' Homologous region	ATCGGAATTCCGCGGAA GTTGGGGAGCACAGAAG	ATCGGAATTCGGGAACACT GGGGTTGAA
3' Homologous region	ATCGGAATTCTCACAGG TTCAACCCCAGT	ATCGGGTACCTGAGCAGTG GATACACCTGAA
Screening Primer1	TGCTCCTGCCGAGAAAGTAT (Neo F)	CTATCAGGCCAACCTGTGGT (Gata1 R)
Screening Primer2	GAAGAGGCACTGGGAGTCAG (Gata1 F)	ATTCTCCCACCGTCAGTACG (CreERT2 R)
Guide RNA	**Sequence 5' to 3'**	
Non-Targeting-1	GTTCATTTCCAAGTCCGCTG	
Non-Targeting-3	GTATTACTGATATTGGTGGG	
Non-Targeting-4	TCATGCTTGCTTGGGCAAAA	
SgPU.1-2	GGGTACTGGAGGCACATCCG	
SgPU.1-3	AGACCTGGTGCCCTATGACA	
SgRUNX1-1	GGATGTTCCAGATGGCACTC	
SgRUNX1-2	GGTCATTAAATCTTGCAACC	

Supplemental Table 2: Antibodies

Human	**Fluorescence**	**Cat#**	**Vendor**
CD235a	APC	551336	BD Biosciences
CD71	FITC	334104	BioLegend
CD11b	PE	301305	BioLegend
Mouse	**Fluorescence**	**Cat#**	**Vendor**
CD71	FITC	113806	BioLegend
Ter119	APC	116212	BioLegend
CD44	APC-Cy7	103028	BioLegend
B220	FITC	103206	BioLegend
Gr1	FITC	108406	BioLegend
CD3e	FITC	100306	BioLegend
CD11b	FITC	101205	BioLegend
CD150	APC	115910	BioLegend
CD41	Alexa Fluor 700	133925	BioLegend
CD41	FITC	133904	BioLegend
CD61	APC	104315	BioLegend
FceRIa	FITC	134305	BioLegend
c-Kit	APC	105812	BioLegend
B220	Biotin	13-0452-85	ThermoFisher
CD2	Biotin	100103	BioLegend
CD3	Biotin	100304	BioLegend
CD5	Biotin	100604	Biolegend
CD8a	Biotin	100704	BioLegend
GR1	Biotin	13-5931-85	ThermoFisher
TER119	Biotin	116204	BioLegend
StAV	BV650	405232	BioLegend
c-Kit	APC-Cy7	105825	BioLegend
Sca1	BV421	108128	BioLegend
CD16/32	BV605	563006	BD Biosciences
CD105	PE-Cy7	120410	BioLegend
Sca1	APC	108111	BioLegend
CD16/32	PE-Cy7	101317	BioLegend
CD34	FITC	553733	BD Biosciences
Ter119	eF450	48-5921-82	ThermoFisher
Gr1	eF450	48-5931-80	ThermoFisher
B220	eF450	48-0452-82	ThermoFisher
CD3e	eF450	48-0032-82	ThermoFisher
CD11b	eF450	48-0112-80	ThermoFisher
CD41	eF450	48-0411-82	ThermoFisher
Live/Dead	**Fluorescence**	**Cat#**	**Vendor**
Annexin-V	PE	556421	BD Biosciences
DAPI	Pacific Blue	422801	BioLegend
Zombie Aqua	BV510	423101	Biolegend